

Ultrafast UV–Vis and IR Studies of *p*-Biphenyllyl Acetyl and Carbomethoxy Carbenes

Jin Wang,[†] Gotard Burdzinski,[‡] Jacek Kubicki,[‡] and Matthew S. Platz^{*,†}

Department of Chemistry, The Ohio State University, 100 West 18th Avenue, Columbus, Ohio, 43210, and the Quantum Electronics Laboratory, Faculty of Physics, Adam Mickiewicz University, 85 Umultowska, Poznan 61-614, Poland

Received May 2, 2008; E-mail: platz.1@osu.edu

Abstract: The photochemistry of a *p*-biphenyllyl diazo ester (BpCN₂CO₂CH₃) and diazo ketone (BpCN₂COCH₃) were studied by ultrafast time-resolved UV–vis and IR spectroscopies. The excited states of these diazo compounds were detected and found to decay with lifetimes of less than 300 fs. The diazo ester produces singlet carbene with greater quantum efficiency than the ketone analogue due to competing Wolff rearrangement (WR) in the excited state of the diazo ketone. Carbene BpCCO₂CH₃ has a singlet–triplet gap that is close to zero in cyclohexane, but the triplet is the ground state. The two spin states are in rapid equilibrium in this solvent relative to reaction with cyclohexane. There is (for a carbene) a slow rate of singlet to triplet intersystem crossing (isc) in this solvent because the orthogonal singlet must rotate to a higher energy orientation prior to isc. In acetonitrile and in dichloromethane BpCCO₂CH₃ has a singlet ground state. Ketocarbene BpCCOCH₃ has a singlet ground state in cyclohexane, in dichloromethane, and in acetonitrile and decays by WR to form a ketene detected by ultrafast IR spectroscopy in these solvents. Ketocarbenes have more stable singlet states, relative to carbene esters, because of the superior conjugation of the filled hybrid orbital of the carbene with the π system of the carbonyl group, the same factor that makes methyl ketones more acidic than the analogous esters. The rate of WR of BpCCOCH₃ is faster in cyclohexane than in dichloromethane and acetonitrile because of intimate solute–solvent interactions between the empty p orbital of the carbene and nonbonding electron pairs of heteroatoms of the solvent. These interactions stabilize the carbene and retard the rate of WR.

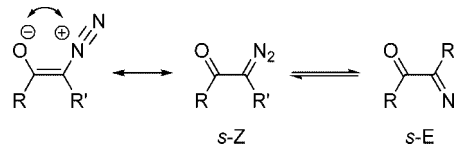
1. Introduction

The conversion of α -diazo ketones into ketenes was discovered in 1902.¹ This reaction, now known as Wolff rearrangement (WR), has been extensively applied in many diverse fields, such as synthetic chemistry, photolithography, and in drug delivery.² Due to the importance of the WR, it has been extensively studied both theoretically and experimentally.

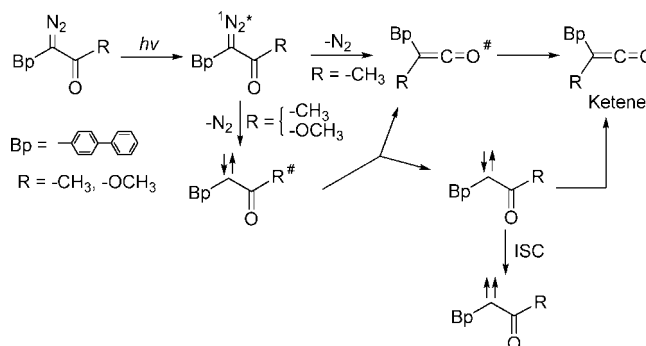
α -Diazo carbonyl compounds usually have a planar configuration of the O=C–C=N₂ group. Rotation around the C–C bond will generate two conformers, *s*-Z and *s*-E as shown in Scheme 1. The C–C bond possesses partial double-bond character in the resonance structure of the *s*-Z conformer (Scheme 1). An attractive interaction between the positively charged nitrogen and the negatively charged oxygen atoms also contributes to the stabilization of the *s*-Z conformer.²

Two mechanisms have been proposed for WR in α -diazo carbonyl compounds (Scheme 2).² One pathway is a concerted mechanism in which the migrating group moves as the dinitrogen is extruded. The other possibility is a stepwise mechanism, in which the diazo compound loses nitrogen to form the carbene and, subsequently, the carbene undergoes WR to form a ketene and/or undergoes bimolecular reactions. In 1966,

Scheme 1. *s*-Z and *s*-E Conformers for α -Diazo Carbonyl Compounds



Scheme 2. Proposed Reaction Pathways for *p*-Biphenyllyl Diazo Ketone and Ester



Kaplan and Meloy³ proposed that ketene formation is favored upon decomposition of the *s*-Z conformer of α -carbonyl

[†] The Ohio State University.



[‡] Adam Mickiewicz University.

(1) Wolff, L. *Justus Liebigs Ann. Chem.* **1902**, 325, 129–195.

(2) Kirmse, W. *Eur. J. Org. Chem.* **2002**, 2193–2256.

(3) Kaplan, F.; Meloy, G. K. *J. Am. Chem. Soc.* **1966**, 88, 950–956.

Table 1. B3LYP/6-311+G(d,p)//B3LYP/6-31G(d) Calculations of Gibbs Free Energy Differences (kcal·mol⁻¹) for syn and anti Conformers of BpCN₂CO₂CH₃ and BpCN₂COCH₃ in the Gas Phase, Cyclohexane, Dichloromethane, and Acetonitrile^a

							
	ΔG_{298K}	syn %	anti %		ΔG_{298K}	syn %	anti %
gas phase ^b	-1.81	4	96		-1.15	13	87
cyclohexane ^c	-1.58	6	94		-0.83	20	80
dichloromethane ^c	-1.14	13	87		-0.27	39	61
acetonitrile ^c	-1.03	15	85		-0.09	46	54

^a Bp = *p*-biphenyl. ^b The zero-point energy (ZPE) for the gas-phase calculations is corrected by a factor of 0.9806. ^c The solution-phase calculations used PCM models, and the geometries are from the gas-phase B3LYP/6-31(d) calculations.

compounds. In contrast, it was proposed that *s-E* conformers preferentially decompose to form *trappable* carbenes. This rule has been supported by numerous experiments.²

The structures of carbonyl-substituted carbenes in their singlet and triplet states have been thoroughly studied by modern theoretical methods.⁴ Triplet acetylcarbene and carbomethoxycarbene are lower in energy than the most stable singlet state. Simple triplet carbonyl carbenes are predicted to have the carbonyl group reside in the same plane as that defined by the carbene carbon and the two atoms to which it is directly bound. The story is quite different in simple singlet carbonyl carbenes in which the carbonyl group is nearly orthogonal to the plane of the carbene carbon and its two directly bonded atomic substituents. Singlet carbenes adopt this conformation to allow the filled hybrid orbital of the carbene to interact with the π^* system of the carbonyl group. This provides the same type of stabilization present in enolate ions.

The Wolff rearrangement of carbonyl carbenes has also received considerable study.⁴ The potential energy surface of acetyl carbene is rather flat. Acetyl carbene rapidly interconverts with the isomeric oxirene and rearranges to ketene over a small (2.7–6.3 kcal/mol) barrier. In the case of carbomethoxycarbene the barrier to Wolff rearrangement was predicted to be between 2.4 and 7.2 kcal/mol, or similar to that of acetylcarbene. Halogen substituents on the carbene center stabilize the singlet relative to the triplet state. In these carbenes the singlet is predicted to be the ground state, and the barrier to Wolff rearrangement of chlorocarbomethoxy carbene increases to 13.9 kcal/mol.

Diazo esters and ketones are also known to experience different photochemistry.² Wang et al.⁵ studied 2-NpCN₂CO₂CH₃ using nanosecond time-resolved infrared spectroscopy and found that the formation of ketene solely arises from the carbene, indicating a stepwise mechanism. The Tomioka group⁶ investigated the photochemistry of PhCN₂CO₂CH₃ and found that photolysis of this diazo compound in neat alcohols does not afford any WR-derived product. This observation again indicates that the concerted mechanism of WR is not operative upon photolysis of the parent diazo ester, PhCN₂CO₂CH₃.

Tomioka et al.⁷ studied the photochemistry of the related diazo ketone, PhCN₂COCH₃, and found that even in methanol, an excellent carbene trap, the WR-derived product cannot be

suppressed. They proposed a concerted mechanism in which ketene formation proceeds from the excited state of the diazo precursor without intervention of a carbene. This is an example of a “rearrangement in the excited state” (RIES) mechanism. Another possibility, which was not considered by the authors, is that ketene formation may involve a stepwise mechanism and arise from very short-lived “hot” carbenes (Scheme 2). Upon photolysis of the diazo ketone, it can decompose to form carbenes with excess vibrational energy. These “hot” ketocarbenes can rapidly overcome the barrier for WR to form ketenes before they thermalize or react with solvents.

Assuming that the conformational differences between the phenyl diazo ketone and ester are slight, Tomioka's⁷ studies illustrate that the Kaplan and Meloy³ rules are difficult to apply to photochemical reactions. In a photochemical experiment both syn and anti conformers are excited, but theory has not yet predicted whether or not excited syn or anti conformers decompose more or less rapidly than they undergo interconversion. One cannot expect the Kaplan and Meloy³ rules to apply if indeed conformational interconversion is rapid on excited-state surfaces.

In this paper, we will discuss the application of state of the art ultrafast time-resolved laser spectroscopy with UV–vis and IR detection methods to investigate the photochemistry of a biphenyl diazo ketone and a biphenyl diazo ester. We will try to distinguish the RIES mechanism from the “hot carbene mechanism”. In addition, WR of ketocarbenes will be found to proceed within 1 ns in fluid solution. Some ketocarbene lifetimes have been indirectly measured by the pyridine ylide method with the aid of various assumptions.^{8–10} In this study, we are able to directly monitor the carbene decay and measure the rate of WR in various solvents.

2. Ultrafast Spectroscopic Results

p-Biphenyl diazo compounds are studied instead of the parent phenyl compounds because the diazo excited states and carbenes absorb at longer wavelengths than the phenyl analogues and as a result are more easily studied in the polycyclic aromatic systems. First, the ground-state geometries of BpCN₂CO₂CH₃ and BpCN₂COCH₃ were calculated in the gas phase and in several solvents. The results are collected in Table 1 and predict that anti rotomers of the ester and ketone will predominate in

(4) Scott, A. P.; Platz, M. S.; Radom, L. *J. Am. Chem. Soc.* **2001**, *123*, 6069–6076.

(5) Wang, Y.; Yuzawa, T.; Hamaguchi, H.-o.; Toscano, J. P. *J. Am. Chem. Soc.* **1999**, *121*, 2875–2882.

(6) Fujiwara, Y.; Tanimoto, Y.; Itoh, M.; Hirai, K.; Tomioka, H. *J. Am. Chem. Soc.* **1987**, *109*, 1942–1946.

(7) Tomioka, H.; Okuno, H.; Kondo, S.; Izawa, Y. *J. Am. Chem. Soc.* **1980**, *102*, 7123–7125.

(8) Wang, J.-L.; Toscano, J. P.; Platz, M. S.; Nikolaev, V.; Popik, V. *J. Am. Chem. Soc.* **1995**, *117*, 5477–5483.

(9) Toscano, J. P.; Platz, M. S.; Nikolaev, V. *J. Am. Chem. Soc.* **1995**, *117*, 4712–4713.

(10) Toscano, J. P.; Platz, M. S.; Nikolaev, V.; Popic, V. *J. Am. Chem. Soc.* **1994**, *116*, 8146–8151.

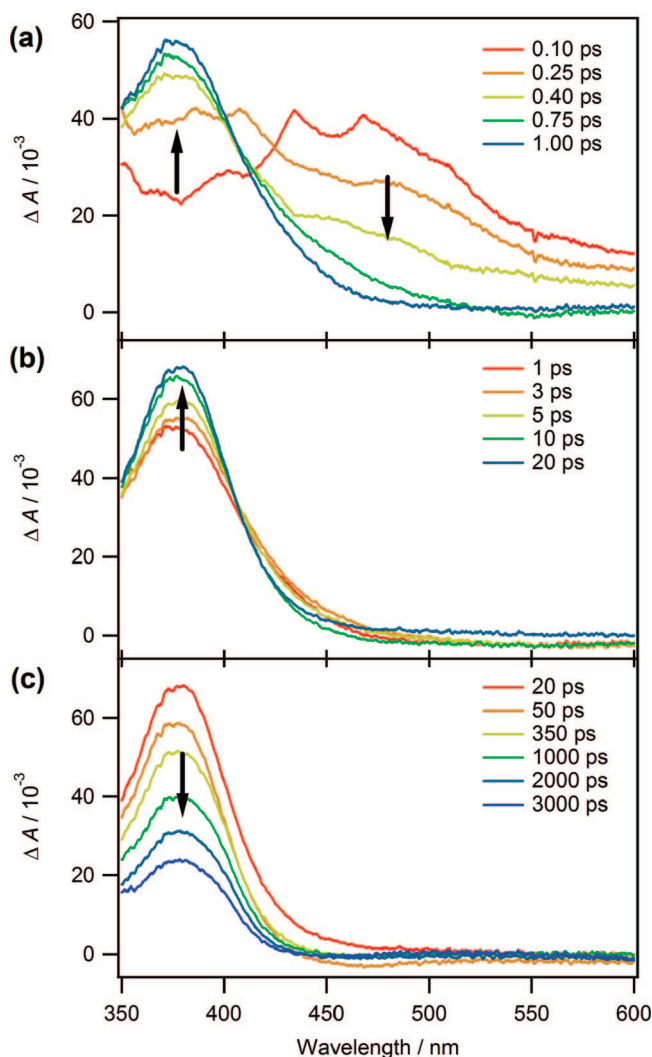


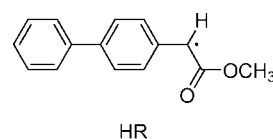
Figure 1. Transient spectra produced by ultrafast photolysis of $\text{BpCN}_2\text{CO}_2\text{CH}_3$ in cyclohexane. The spectra were generated by ultrafast LFP ($\lambda_{\text{ex}} = 308 \text{ nm}$) with time windows of (a) 0.10–1.00 ps, (b) 1–20 ps, and (c) 20–3000 ps.

all solvents under study. Thus, differences in the photochemistries of the diazo ester and ketone will not be due to differences in their *ground-state* geometries. We note that NMR analysis of both diazo compounds is consistent with rapid interconversion; thus, the barriers connecting the rotomers are small and are likely in the range of 13–16 kcal/mol observed with similar compounds.²

2.1. Weakly Coordinating Solvents. Ultrafast photolysis ($\lambda_{\text{ex}} = 308 \text{ nm}$) of $\text{BpCN}_2\text{CO}_2\text{CH}_3$ in cyclohexane produces the transient spectra shown in Figure 1. A broadly absorbing transient with absorption maximum at 475 nm is formed within the laser pulse and decays in 300 fs. As this transient absorption decays, a new transient is observed with $\lambda_{\text{max}} = 375 \text{ nm}$. Following our previous studies,^{11–18} the former band is attributed to an excited state of the diazo precursor $^1\text{BpCN}_2\text{CO}_2\text{CH}_3^*$ and

the latter to singlet carbene ester $^1\text{BpCCO}_2\text{CH}_3$. Time-dependent density functional theory (TD-DFT) calculations predict that $^1\text{BpCCO}_2\text{CH}_3$ absorbs at 368 nm ($f = 0.4569$, Table S1), in excellent agreement with the experimental results. The absorption band of $^1\text{BpCCO}_2\text{CH}_3$ sharpens with a time constant of 5.5 ps and decays biexponentially with time constants of $20 \pm 3 \text{ ps}$ and a few nanoseconds (Figure S1a). The fast components (5.5 and 20 ps) are assigned to vibrational cooling of the hot carbene.^{12,19–23} We speculate that the growth of the $^1\text{BpCCO}_2\text{CH}_3$ signal is due to different oscillator strengths of the vibrationally hot and the thermalized carbene.²⁴ The slow component is assigned to the intrinsic lifetime for the relaxed singlet carbene, but its lifetime cannot be measured accurately with our ultrafast spectrometer. Thus, our best estimate of τ of the relaxed carbene is $\sim 2 \text{ ns}$ in cyclohexane.

Nanosecond (ns) laser flash photolysis (LFP) ($\lambda_{\text{ex}} = 308 \text{ nm}$) studies were performed to determine the ground-state multiplicity of $\text{BpCCO}_2\text{CH}_3$ in argon-saturated cyclohexane, and the spectra are shown in Figure S2. A transient absorption band absorbing between 320 and 400 nm is observed 10 ns after the laser pulse and decays with a time constant of 49 ns (Figure S3a). A new transient, centered at 335 nm, can be observed 1 μs after the laser pulse, which decays biexponentially with time constants of 20 and 90 μs (Figure S3b). The initially observed transient on the nanosecond time scale (red spectrum of Figure S2) is assigned to the triplet state of the carbene ($^3\text{BpCCO}_2\text{CH}_3$), and the transient observed at longer delay times (blue spectrum of Figure S2) is assigned to the radical HR, formed by hydrogen atom abstraction by the triplet carbene from the solvent. TD-DFT calculations predict that $^3\text{BpCCO}_2\text{CH}_3$ and radical HR absorb at 353 nm ($f = 0.5330$, Table S2) and 358 nm ($f = 0.4736$, Table S3), respectively, in good agreement with the experimental results.

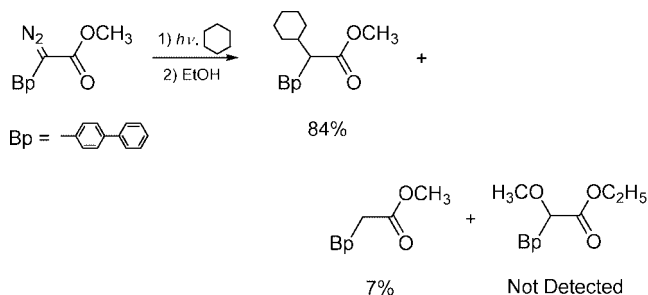


It is interesting to note that there is a shoulder accompanying the triplet carbene transient absorption band, from 370 to 430 nm (red spectrum of Figure S2). This shoulder (spectral feature) decays with the same rate as the triplet carbene. We posit that this shoulder feature of the spectrum can be assigned to the singlet carbene because it is similar to the singlet carbene absorption obtained by ultrafast photolysis (Figure 1). Since the absorption coefficients of singlet and triplet $\text{BpCCO}_2\text{CH}_3$ are

- (11) Wang, J.; Burdzinski, G.; Gustafson, T. L.; Platz, M. S. *J. Org. Chem.* **2006**, *71*, 6221–6228.
- (12) Wang, J.; Burdzinski, G.; Gustafson, T. L.; Platz, M. S. *J. Am. Chem. Soc.* **2007**, *129*, 2597–2606.
- (13) Wang, J.; Kubicki, J.; Hilinski, E. F.; Mecklenburg, S. L.; Gustafson, T. L.; Platz, M. S. *J. Am. Chem. Soc.* **2007**, *129*, 13683–13690.
- (14) Burdzinski, G.; Wang, J.; Gustafson, T. L.; Platz, M. S. *J. Am. Chem. Soc.* **2008**, *130*, 3746–3747.

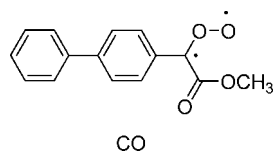
- (15) Wang, J.; Burdzinski, G.; Kubicki, J.; Gustafson, T. L.; Platz, M. S. *J. Am. Chem. Soc.* **2008**, *130*, 5418–5419.
- (16) Wang, J.; Kubicki, J.; Gustafson, T. L.; Platz, M. S. *J. Am. Chem. Soc.* **2008**, *130*, 2304–2313.
- (17) Wang, J.; Kubicki, J.; Peng, H.; Platz, M. S. *J. Am. Chem. Soc.* **2008**, *130*, 6604–6609.
- (18) Wang, J.; Zhang, Y.; Kubicki, J.; Platz, M. S. *Photochem. Photobiol. Sci.* **2008**, *7*, 552–557.
- (19) Laermer, F.; Elsaesser, T.; Kaiser, W. *Chem. Phys. Lett.* **1989**, *156*, 381–386.
- (20) Miyasaka, H.; Hagihara, M.; Okada, T.; Mataga, N. *Chem. Phys. Lett.* **1992**, *188*, 259–264.
- (21) Schwarzer, D.; Troe, J.; Votsmeier, M.; Zerezke, M. *J. Chem. Phys.* **1996**, *105*, 3121–3131.
- (22) Elsaesser, T.; Kaiser, W. *Annu. Rev. Phys. Chem.* **1991**, *42*, 83–107.
- (23) Burdzinski, G.; Hackett, J. C.; Wang, J.; Gustafson, T. L.; Hadad, C. M.; Platz, M. S. *J. Am. Chem. Soc.* **2006**, *128*, 13402–13411.
- (24) Mohammed, O. F.; Vauthey, E. *J. Phys. Chem. A* **2008**, *112*, 3823–3830.

Scheme 3. Product Studies of Photolysis (308 nm) of $\text{BpCN}_2\text{CO}_2\text{CH}_3$ in Cyclohexane



not known, we cannot deduce the yields of the singlet and triplet carbenes and the singlet–triplet (S–T) gap. However, ΔG_{ST} must be within $\pm 1 \text{ kcal}\cdot\text{mol}^{-1}$ at 298 K in cyclohexane to allow us to simultaneously detect both spin isomers. Note that at 298 K, a $1 \text{ kcal}\cdot\text{mol}^{-1}$ of the carbene S–T gap corresponds to a spin equilibrium mixture containing 16% of one spin isomer and 84% of the other. We will later provide evidence that the triplet is the ground state of the carbene in cyclohexane and that the slow intersystem crossing (isc) rate is due to the difference in singlet and triplet geometries.

When the cyclohexane solution was saturated with oxygen, dramatically different results were obtained (Figure S4). Again, the triplet carbene $^3\text{BpCCO}_2\text{CH}_3$ absorption spectrum was observed in the region between 320 and 400 nm, 10 ns after the laser pulse, but in the presence of oxygen the triplet lifetime is shortened to 25 ns (Figure S5). The long component (340 ns) of the kinetic trace probed at 335 nm is assigned to radical HR. However, $1 \mu\text{s}$ after the laser pulse, a new band centered at 425 nm was generated in the oxygen-saturated solution, which is strikingly different from the results obtained in argon-saturated cyclohexane solution. The lifetime of this species is greater than 200 μs . Following Tomioka's studies,⁶ the carrier of transient absorption centered at 425 nm is assigned to the carbene carbonyl oxide CO.



Very similar ultrafast results were obtained in cyclohexane- d_{12} . The singlet carbene has the same lifetime in cyclohexane- d_{12} (Figure S1b) as in cyclohexane. Clearly, the lifetime of $^1\text{BpCCO}_2\text{CH}_3$ in cyclohexane is not controlled by reaction with solvent and must be controlled instead by a unimolecular process, either WR or isc.

To better appreciate the sign and magnitude of ΔG_{ST} in cyclohexane, $\text{BpCN}_2\text{CO}_2\text{CH}_3$ ($\sim 1 \text{ mg/mL}$) was photolyzed ($\lambda_{\text{ex}} = 308 \text{ nm}$) in cyclohexane. After the photolysis was complete, ethanol was added to quench formation of the ketene reaction products. The reaction mixture was analyzed by NMR and gas chromatography–mass spectrometry (GC–MS) (cf., the Experimental Section for details of product studies), and the results of this product study are shown in Scheme 3. The major product is the cyclohexane C–H insertion product (84%). The triplet carbene double hydrogen abstraction product can also be observed (7%) along with bicyclohexane (due to the combination of two cyclohexyl radicals). Interestingly, the WR product does not form to an appreciable extent and cannot be detected

by GC–MS, indicating that the unimolecular decay of $^1\text{BpCCO}_2\text{CH}_3$ in cyclohexane (vide supra) is mainly controlled by isc to form a spin equilibrium mixture rather than WR.

The analogous photolysis of $\text{BpCN}_2\text{CO}_2\text{CH}_3$ was performed in a 1:1 mixture of cyclohexane and cyclohexane- d_{12} . Analyzing the cyclohexane C–H/C–D insertion product ratio, we deduce a kinetic isotope effect of 2.5, which is consistent with the previously reported values of singlet carbene insertion reactions.^{25,26} Since $^1\text{BpCCO}_2\text{CH}_3$ decays with the same rate in cyclohexane and in cyclohexane- d_{12} , the C–H insertion product must be formed from the carbene singlet–triplet equilibrium mixture. The absence of ketene-derived product indicates that the spin equilibrated carbene does not undergo WR in cyclohexane even on a time scale of tens of nanoseconds.

The absorption of $^1\text{BpCCO}_2\text{CH}_3$ at 3 ns is $\sim 35\%$ of its maximum absorption determined 20 ps after the laser pulse (Figure 1c). Since the decay of $^1\text{BpCCO}_2\text{CH}_3$ is mainly controlled by isc, it can be deduced that in the S–T equilibrium mixture there is no less than 65% of $^3\text{BpCCO}_2\text{CH}_3$ and no more than 35% of $^1\text{BpCCO}_2\text{CH}_3$ present, which corresponds to an equilibrium constant $K_{\text{eq}} = [^3\text{BpCCO}_2\text{CH}_3]_{\text{eq}}/[^1\text{BpCCO}_2\text{CH}_3]_{\text{eq}} \geq 1.86$, where $[^1\text{BpCCO}_2\text{CH}_3]_{\text{eq}}$ and $[^3\text{BpCCO}_2\text{CH}_3]_{\text{eq}}$ are the singlet and triplet carbene concentrations at equilibrium, and the S–T energy gap $\Delta G_{\text{ST}} \geq 0.4 \text{ kcal}\cdot\text{mol}^{-1}$. Combining our previous analysis that ΔG_{ST} is within $\pm 1 \text{ kcal}\cdot\text{mol}^{-1}$, we conclude that ΔG_{ST} is within $0.4\text{--}1 \text{ kcal}\cdot\text{mol}^{-1}$ and that $^3\text{BpCCO}_2\text{CH}_3$ is the ground state in cyclohexane.

The lifetime of $^1\text{BpCCO}_2\text{CH}_3$ shortens to $1.2 \pm 0.1 \text{ ns}$ in cyclohexene (Figure S6). In neat alkene, the carbene ester reacts with solvent in competition with unimolecular decay by isc, presumably to form cyclopropanes.

Ultrafast photolysis of diazoketone $\text{BpCN}_2\text{COCH}_3$ produces the transient spectra shown in Figure 2. The excited state, $^1\text{BpCN}_2\text{COCH}_3^*$, is the first species observed in the visible region, and it decays within the instrument response time (300 fs) to form singlet ketocarbene with $\lambda_{\text{max}} = 365 \text{ nm}$. TD-DFT calculations predict that $^1\text{BpCCOCH}_3$ absorbs at 348 nm ($f = 0.5041$, Table S4), in good agreement with the experimental results. The transient absorption in the region of 420 and 550 nm observed at longer delay times (Figure 2b) is due to the re-excitation of the photoproduct ketene (cf., the Experimental Section). Vibrational cooling (VC) of the carbene is observed and has a time constant of $11 \pm 3 \text{ ps}$ (Figure S7). The relaxed ketocarbene decays an order of magnitude more rapidly in cyclohexane ($\tau = 180 \pm 20 \text{ ps}$, Figure S7) than the analogous carbene ester (Figure S1). The lifetime of the relaxed ketocarbene $^1\text{BpCCOCH}_3$ is the same in cyclohexane, cyclohexane- d_{12} (Figure S7b), and in cyclohexene (Figure S8). This demonstrates that the lifetime of $^1\text{BpCOCH}_3$ is controlled by a very rapid unimolecular processes, even in the more reactive alkene solvent.

Nanosecond LFP studies were also performed for $\text{BpCN}_2\text{COCH}_3$ in argon-saturated cyclohexane. We could not observe any spectral signatures of the triplet ketocarbene $^3\text{BpCCOCH}_3$. It is possible that a transient is hidden in the bleaching region of $\text{BpCN}_2\text{COCH}_3$ that is centered at 300 nm. The transient spectra observed centered at 300 nm does not decay on a time window of 500 μs . We tentatively assign this transient to the ketene, formed by WR of the carbene. This assignment is also

- (25) Barcus, R. L.; Hadel, L. M.; Johnston, L. J.; Platz, M. S.; Savino, T. G.; Scaiano, J. C. *J. Am. Chem. Soc.* **1986**, *108*, 3928–3937.
 (26) Platz, M.; Admasu, A. S.; Kwiatkowski, S.; Crocker, P. J.; Imai, N.; Watt, D. S. *Bioconjugate Chem.* **1991**, *2*, 337–341.

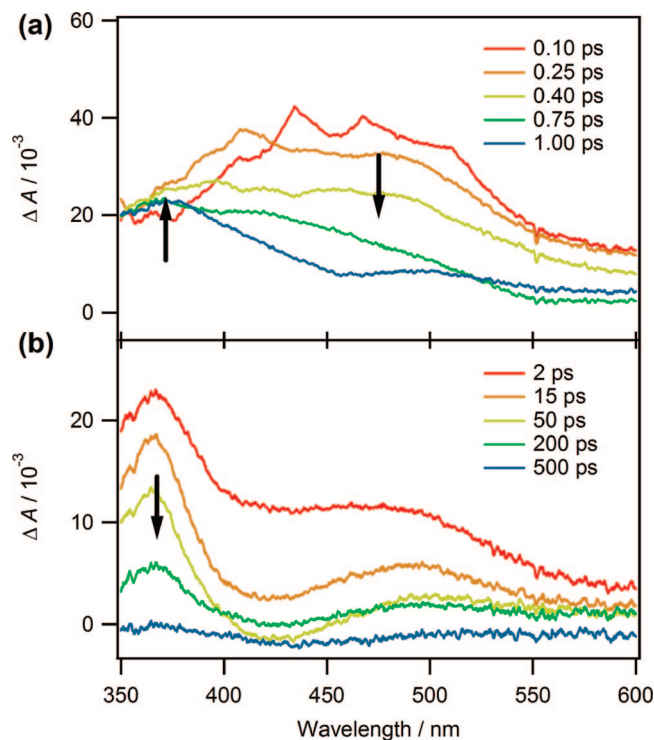


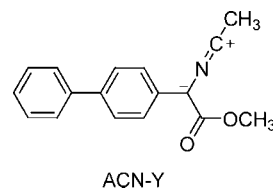
Figure 2. Transient spectra produced by ultrafast photolysis of $\text{BpCN}_2\text{COCH}_3$ in cyclohexane. The spectra were generated by ultrafast LFP ($\lambda_{\text{ex}} = 308 \text{ nm}$) with time windows of (a) 0.10–1.00 ps and (b) 2–500 ps.

in accord with TD-DFT calculations for the ketene ($\lambda_{\text{max}} = 302 \text{ nm}$, $f = 0.6321$, Table S5).

A comparison of the two figures in Figure 3 reveals that the optical yield of ketocarbene is consistently less than half of that of the carbene ester, a trend which is found in other solvents as well (Table 3). These experiments were performed on the same day, using the same optical alignment of the spectrometer and utilized solutions of equal diazo absorbance at the wavelength of excitation (308 nm). This is reminiscent of our ultrafast studies of 1,2 hydrogen shift in the diazo excited states.¹² Following our previous study¹² and a large body of literature,² we propose that the difference of the optical yields of the two initially formed carbonyl carbenes is due to the fact that WR proceeds efficiently in the diazo excited state of $\text{BpCN}_2\text{COCH}_3$ but is not a major deactivation pathway for the excited state of $\text{BpCN}_2\text{CO}_2\text{CH}_3$. A more detailed discussion will be given in section 3.1.

2.2. Coordinating Solvents. 2.2.1. Acetonitrile. The photochemistries of $\text{BpCN}_2\text{COCH}_3$ and $\text{BpCN}_2\text{CO}_2\text{CH}_3$ were also studied in acetonitrile (ACN). The results are given in Figures 4 and 5. Excited diazo compounds, singlet carbenes, and VC/solvation dynamics are observed along with transients formed by re-excitation of persistent photoproducts in the region of 480 nm for $\text{BpCN}_2\text{CO}_2\text{CH}_3$, and 440 and 500 nm for $\text{BpCN}_2\text{COCH}_3$ (cf., the Experimental Section for more details). The lifetime of singlet carbene ester $^1\text{BpCCO}_2\text{CH}_3$ ($\lambda_{\text{max}} = 400 \text{ nm}$) exceeds 3 ns in acetonitrile and cannot be determined by ultrafast methods. With the use of ns time-resolved laser flash photolysis methods, the lifetime of $^1\text{BpCCO}_2\text{CH}_3$ is determined as 180 ns (left panel of Figure S10), and there is no oxygen effect observed on the lifetime, which proves that the observed transient is not a triplet carbene. This observation also demonstrates that the carrier of the transient absorption is not in rapid equilibrium with an accessible oxygen-sensitive species. As the decay of

$^1\text{BpCCO}_2\text{CH}_3$ proceeds, a rising absorption centered at 340 nm with a similar time constant ($\tau = 120 \text{ ns}$, right panel of Figure S10) is observed. The 340 nm absorbing species overlaps severely with the spectrum of $^1\text{BpCCO}_2\text{CH}_3$ (Figure S11); thus, the decay time constant of $^1\text{BpCCO}_2\text{CH}_3$ appears to differ somewhat from the rise time constant of the 340 nm absorption band because of the spectral interference. The lifetime of the 340 nm transient is 115 μs (Figure S12), and again, there is no oxygen effect on the lifetime. Following previous studies, this 340 nm transient absorption is assigned to the $^1\text{BpCCO}_2\text{CH}_3$ –acetonitrile ylide ACN-Y . TD-DFT predicts that the acetonitrile ylide absorbs at 367 nm ($f = 0.4569$, Table S6), in good agreement with the experimental results. Furthermore, on the basis of the lifetime of $^1\text{BpCCO}_2\text{CH}_3$ (180 ns), the absence of an oxygen effect on the lifetime, and the lack of a spectral signature for $^3\text{BpCCO}_2\text{CH}_3$, we conclude that $^1\text{BpCCO}_2\text{CH}_3$ is the ground state of the carbene in acetonitrile.



The lifetime of the ketocarbene is $700 \pm 30 \text{ ps}$ in acetonitrile (Figure S13a). This is much shorter than that of the carbene ester but is much longer than the lifetime of the ketocarbene in cyclohexane. The ketocarbene lifetime in acetonitrile- d_3 (Figure S13b) is the same as in acetonitrile indicating that the decay of $^1\text{BpCCOCH}_3$ in this solvent is unimolecular and most likely due to WR as a nitrile ylide is not observed.

Nanosecond LFP (308 nm) of $\text{BpCN}_2\text{COCH}_3$ in acetonitrile produces results similar to those obtained in cyclohexane. Neither $^3\text{BpCCOCH}_3$ nor the acetonitrile ylide is observed. The only transient observed is the ketene, formed by WR, which does not decay over a 500 μs time window.

Ultrafast photolysis of $\text{BpCN}_2\text{COCH}_3$ ($\lambda_{\text{ex}} = 270 \text{ nm}$) with IR detection was also performed in acetonitrile (Figure 6). In the region of 2060–2140 cm^{-1} , the diazo bleaching band (2076 cm^{-1}) is observed immediately after the laser pulse (300 fs). The ketene K band (2100 cm^{-1}) is also observed immediately ($\tau < 0.4 \text{ ps}$) after the laser pulse.^{14,15} The band narrows and blue-shifts over 30 ps and then grows further over 700 ps (Figure S14). The ketene is formed initially hot, and its band blue-shifts and narrows 50 ps after the laser pulse. It is possible that the ketene is formed by rearrangement of the hot singlet carbene $^1\text{BpCCOCH}_3^\#$. Alternatively, the hot ketene can be formed by WR in the diazo excited state without intervention of the carbene. We are leaning toward the latter explanation for reasons detailed in section 3.1.

2.2.2. Alcohols. Ultrafast time-resolved studies were also performed in methanol. Interestingly, the transient absorption spectra of $^1\text{BpCCOCH}_3$ and $^1\text{BpCCO}_2\text{CH}_3$ shift to longer wavelengths between 1–25 ps after the laser flash. This is not due to VC which typically involves a blue shift. This pattern was first reported with $^1\text{BpCCF}_3$ and was interpreted as the dynamics of solvation of the singlet carbene (Scheme 4).¹⁶

As these singlet carbenes have zwitterionic, closed-shell electronic structures, one expects that the empty p orbital of the carbene will interact with nonbonding electrons on oxygen and that the hydroxyl proton will interact with the filled, in-plane hybrid orbital of the ester carbene. The lifetimes of the

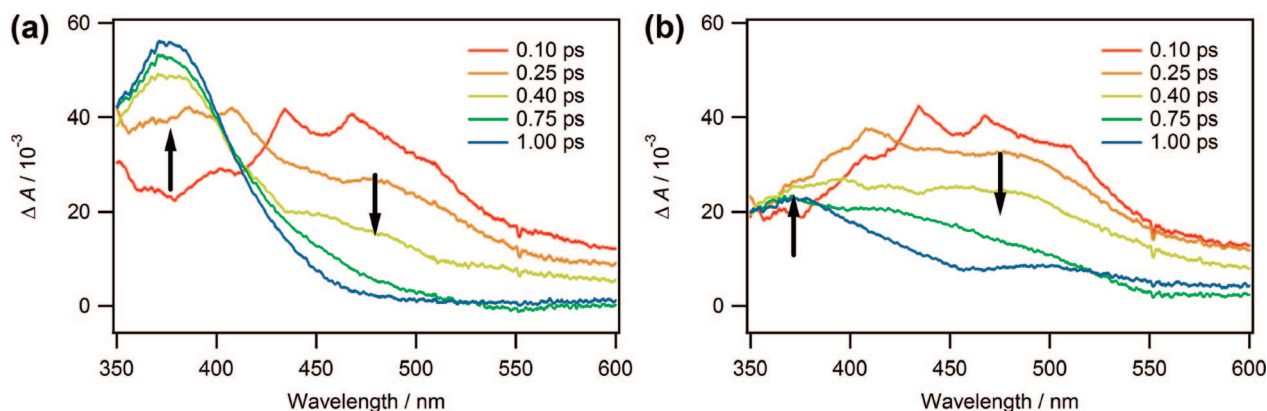


Figure 3. Transient spectra produced by ultrafast photolysis of (a) BpCN₂CO₂CH₃ and (b) BpCN₂COCH₃ in cyclohexane. The spectra were generated by ultrafast LFP ($\lambda_{\text{ex}} = 308$ nm) with a time window of 0.10–1.00 ps.

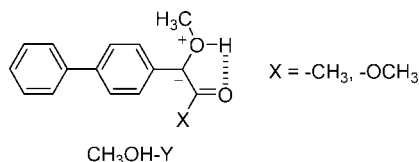
Table 2. Lifetimes and Spectral λ_{max} Shifts of Carbenes ¹BpCCO₂CH₃ and ¹BpCCOCH₃ in Various Solvents

	¹ BpCCO ₂ CH ₃			¹ BpCCOCH ₃		
	$\tau_{\text{obs}}/\text{ns}^a$	$\lambda_{\text{initial}}/\text{nm}$	$\lambda_{\text{final}}/\text{nm}$	$\tau_{\text{obs}}/\text{ps}$	$\lambda_{\text{initial}}/\text{nm}$	$\lambda_{\text{final}}/\text{nm}$
cyclohexane	$\sim 2^b$	375	375	180 ± 20	365	365
cyclohexane- <i>d</i> ₁₂	$\sim 2^b$	375	375	200 ± 30	365	365
cyclohexene	1.2 ± 0.1	385	385	170 ± 10	375	375
acetonitrile	180 ± 20	400	400	700 ± 30	380	380
acetonitrile- <i>d</i> ₃				680 ± 30	380	380
methanol	$(185 \pm 7) \times 10^{-3}$	390	410	120 ± 10	390	395
methanol-OD	$(426 \pm 6) \times 10^{-3}$	390	410	130 ± 10	390	395
TFE ^c	$(20 \pm 2) \times 10^{-3}$	385	415	440 ± 40	420	435
THF ^d	~ 2	375	395	280 ± 20	370	375
diisopropyl ether	~ 5	385	385	310 ± 30	375	375
2-propanol	~ 5	390	410	230 ± 20	380	385
dichloromethane	790 ± 20	400	400	770 ± 40	390	390

^a Most of the lifetimes of ¹Bp-C-CO₂CH₃ are on a nanosecond time scale, except those in methanol, methanol-OD, and TFE. ^b These lifetimes are too long to be accurately measured on our ultrafast spectrometer. But by comparing the kinetic traces, the decay of ¹BpCCO₂CH₃ has a similar rate in cyclohexane and in cyclohexane-*d*₁₂. ^c TFE = 2,2,2-trifluoroethanol. ^d THF = tetrahydrofuran.

carbene ester in methanol and methanol-OD are 185 ± 7 and 426 ± 6 ps, respectively. There is no time-resolved spectroscopic evidence that reaction of the carbene ester with methanol leads to a significant yield of a cation formed by the abstraction of a proton from the solvent. Thus, the kinetic isotope effect (KIE) of 2.3 indicates that the carbene ester primarily reacts with methanol by a concerted insertion of the carbene into an OH bond.

The ketocarbene lifetime is 120 ± 10 ps in methanol and 130 ± 10 ps in methanol-OD. The absence of a KIE, and the lack of spectroscopic evidence of cation formation, persuades us to posit that if ¹BpCCOCH₃ reacts with neat methanol, it proceeds by initial formation of an ylide (CH₃OH-Y) which subsequently forms an ether by a proton shuttle mechanism.²⁷ The putative CH₃OH-Y was not detected by spectroscopic methods.

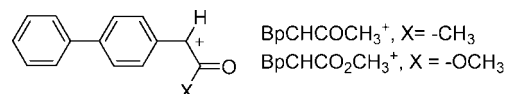


We cannot rule out the possibility that WR of the ketocarbene is faster than reaction with solvent. Given the product study data of Tomioka et al. with PhCCOCH₃,⁷ this interpretation

seems likely and also explains the lack of a KIE on the lifetime of the keto carbene with methanol.

A different story is told in α,α,α -trifluoroethanol (TFE). In the acidic solvent, the decays of both BpCCOCH₃ and BpCCO₂CH₃ are accompanied by the growth of transient absorptions at 490 nm (Figures S15 and S16). These transient absorptions are attributed to cations BpCHCO₂CH₃⁺ and BpCHCOCH₃⁺. The lifetime of ¹BpCCO₂CH₃ is 20 ± 2 ps in TFE, which is obtained by fitting the growth of BpCHCO₂CH₃⁺ (Figure S17). The decay of ¹BpCCO₂CH₃ in TFE is controlled, at least in part, by the cation formation route. The lifetime of cation BpCHCO₂CH₃⁺ in TFE is too long to be accurately measured on our spectrometer, and our best estimate is ~ 2 ns.

The lifetime of ketocarbene ¹BpCCOCH₃ is 440 ± 40 ps in TFE (Figure S18), which is longer than that recorded in methanol (120 ± 10 ps). In methanol, the decay of ketocarbene ¹BpCCOCH₃ is controlled by ylide formation and, more likely, WR. Because TFE is less nucleophilic than methanol the ylide formation reaction pathway will be even less likely than in TFE. The decay of ¹BpCCOCH₃ is controlled, at least in part, by cation formation in TFE. Since the fate of ¹BpCCOCH₃ in TFE is controlled by a different mechanism from that operative in methanol, it is not surprising that ¹BpCCOCH₃ has a different lifetime in TFE than in methanol.



(27) Bethell, D.; Newall, A. R.; Whittaker, D. *J. Chem. Soc., Perkin Trans. 2* 1971, 23–31.

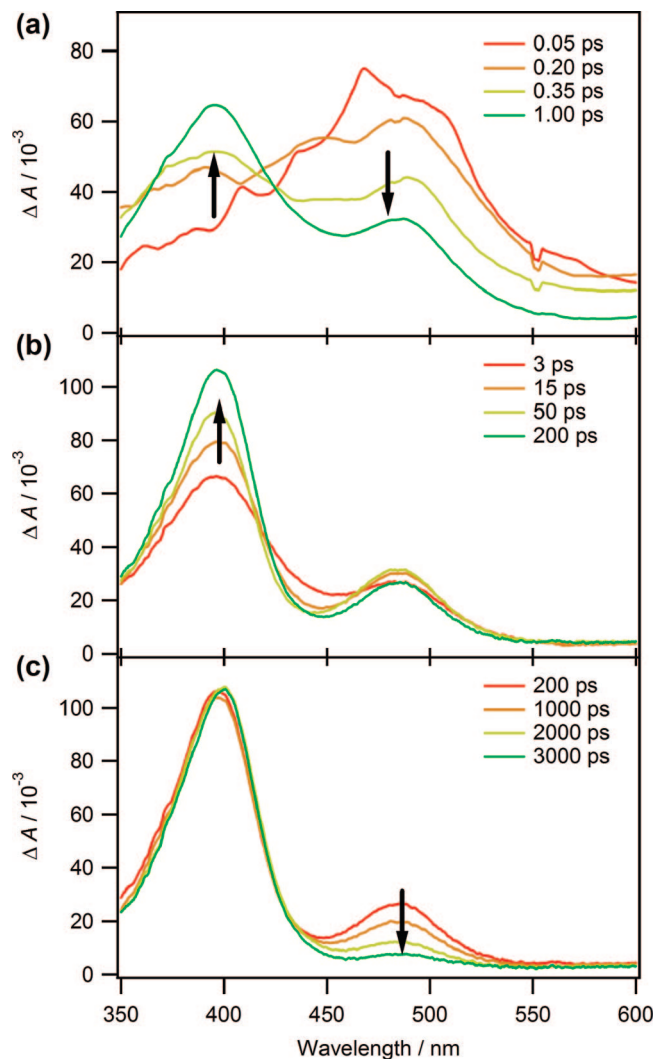


Figure 4. Transient spectra produced by ultrafast photolysis of $\text{BpCN}_2\text{CO}_2\text{CH}_3$ in acetonitrile. The spectra were generated by ultrafast LFP ($\lambda_{\text{ex}} = 308 \text{ nm}$) with time windows of (a) 0.05–1.00 ps, (b) 3–200 ps, and (c) 200–3000 ps.

The lifetimes of the ketocarbene and the carbene ester in methanol are more than an order of magnitude longer than those of singlet diphenylcarbene and *p*-biphenylcarbene in the same solvent. In the latter two carbenes, the proton transfer process is significant. The electron-withdrawing groups acetyl, ester, and of a related, analogous, recently reported system, CF_3 ($\tau = 31 \text{ ps}$),¹⁶ destabilize carbocations and depress the rate of the proton transfer reaction of these types of carbenes with methanol and thus extend the lifetimes of carbenes substituted with electron-withdrawing groups, in methanol. Indeed, the fates of $^1\text{BpCCO}_2\text{CH}_3$ and $^1\text{BpCCOCH}_3$ are mainly controlled by ylide formation and/or O–H insertion mechanisms.

In 2-propanol, a more sterically hindered alcohol, both $^1\text{BpCCO}_2\text{CH}_3$ and $^1\text{BpCCOCH}_3$ display red shifts between 2–20 ps after the laser pulse. The lifetime of $^1\text{BpCCOCH}_3$ in 2-propanol is $230 \pm 20 \text{ ps}$, longer than its lifetime in methanol (120 ps). The lifetime of $^1\text{BpCCO}_2\text{CH}_3$ in 2-propanol is too long to be measured accurately, and the best estimate of its lifetime is $\sim 5 \text{ ns}$.

2.2.3. Ethers. Ultrafast time-resolved studies of $\text{BpCN}_2\text{COCH}_3$ and $\text{BpCN}_2\text{CO}_2\text{CH}_3$ were also performed in tetrahydrofuran (THF). As shown in Figures S19 and S20, the

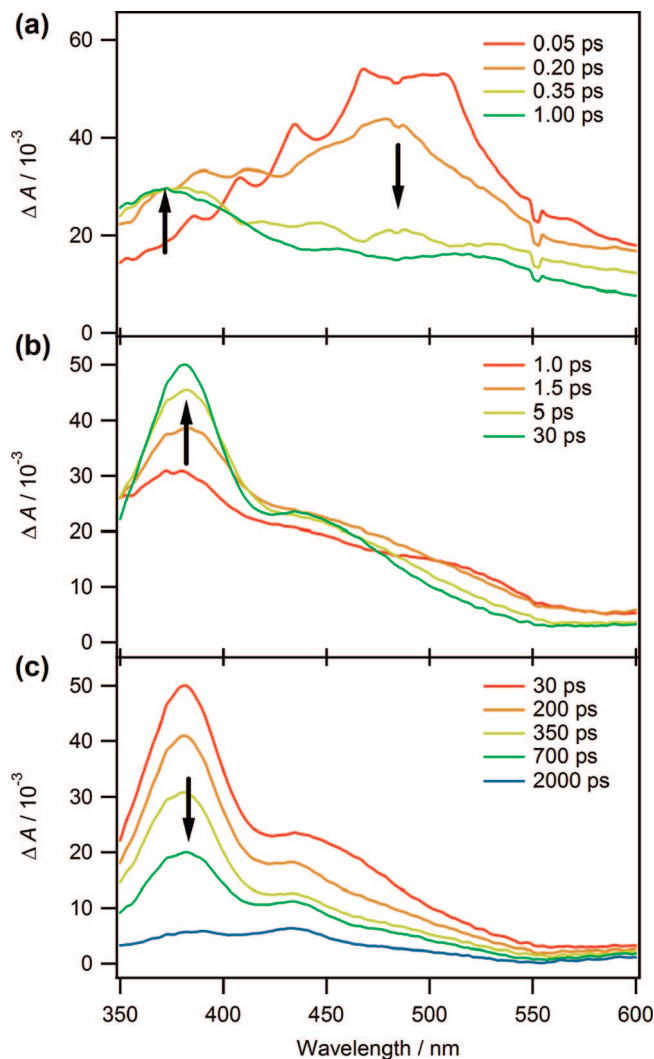


Figure 5. Transient spectra produced by ultrafast photolysis of $\text{BpCN}_2\text{COCH}_3$ in acetonitrile. The spectra were generated by ultrafast LFP ($\lambda_{\text{ex}} = 308 \text{ nm}$) with time windows of (a) 0.05–1.00 ps, (b) 1–30 ps, and (c) 30–2000 ps.

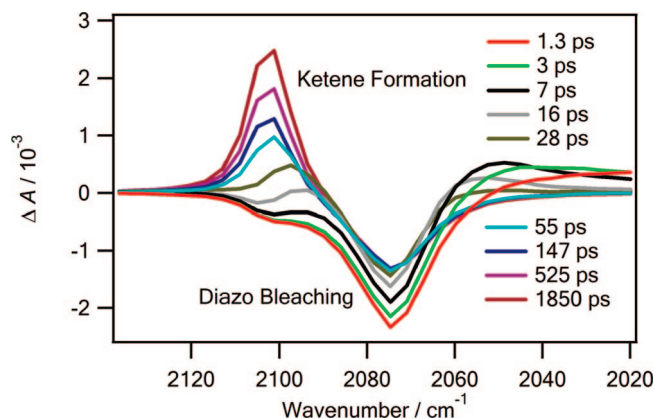


Figure 6. Transient IR spectra produced by ultrafast photolysis of $\text{BpCN}_2\text{COCH}_3$ in acetonitrile. The spectra were generated by ultrafast LFP ($\lambda_{\text{ex}} = 270 \text{ nm}$) with a time window of 1.3–1850 ps.

initially observed transient spectra of the carbene shifts to longer wavelengths between 1–20 ps after the laser pulse. Once again, this is attributed to the dynamics of carbene solvation.¹⁸ The lifetimes of $^1\text{BpCCO}_2\text{CH}_3$ and $^1\text{BpCCOCH}_3$ are ~ 2 (Figure

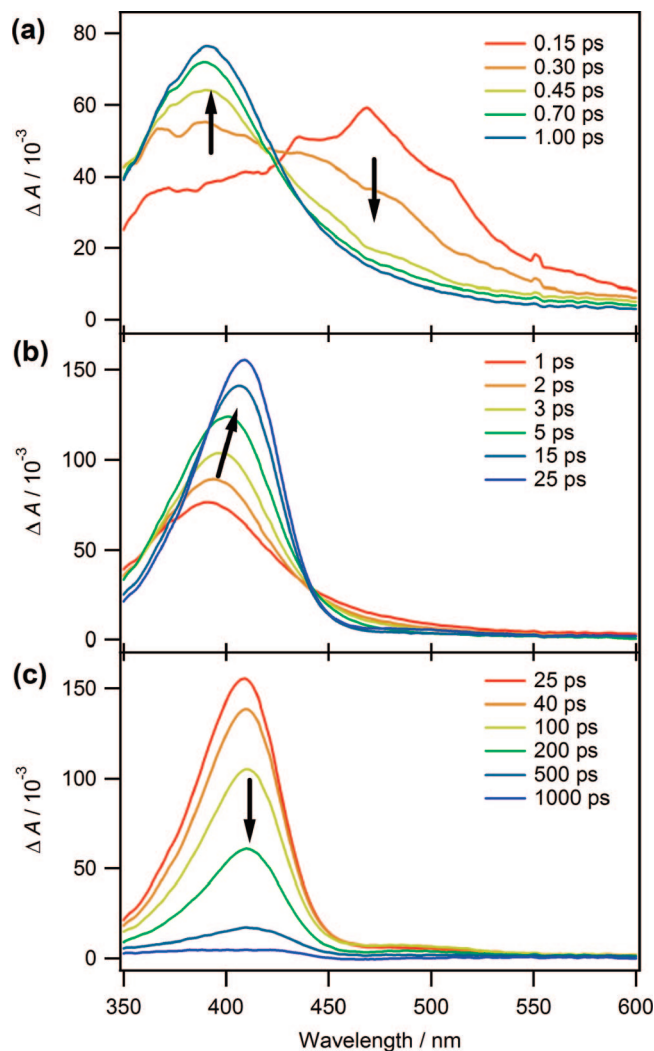
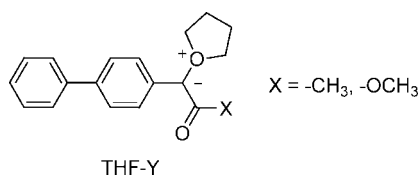


Figure 7. Transient spectra produced by ultrafast photolysis of BpCN₂CO₂CH₃ in methanol. The spectra were generated by ultrafast LFP ($\lambda_{\text{ex}} = 308$ nm) with time windows of (a) 0.10–1.00 ps, (b) 1–25 ps, and (c) 25–1000 ps.

S21) and 0.28 ns (Figure S22), respectively, in THF. As the transient absorption of ¹BpCCO₂CH₃ decays, a transient absorption centered at 360 nm is formed with an isosbestic point at 370 nm (Figure S19b), which is attributed to a THF–carbene ylide THF–Y (X = OCH₃). In the case of ¹BpCCOCH₃, as the singlet carbene decays, the spectral maximum shifts to 365 nm (Figure S20b), which is also assigned to THF–Y (X = CH₃) ylide.



The lifetimes of these ylides were determined by ns time-resolved LFP methods. The lifetime of the ester carbene ylide (X = OCH₃) is 120 μ s in THF (Figure S23). For the ketocarbene ylide (X = CH₃), the lifetime is too long to be determined accurately by our ns spectrometer, and the best estimate of its lifetime is \sim 900 μ s (Figure S24).

TD-DFT methods predict that the THF ylides will have absorption maxima at 342 (X = OCH₃, $f = 0.5172$) and 346

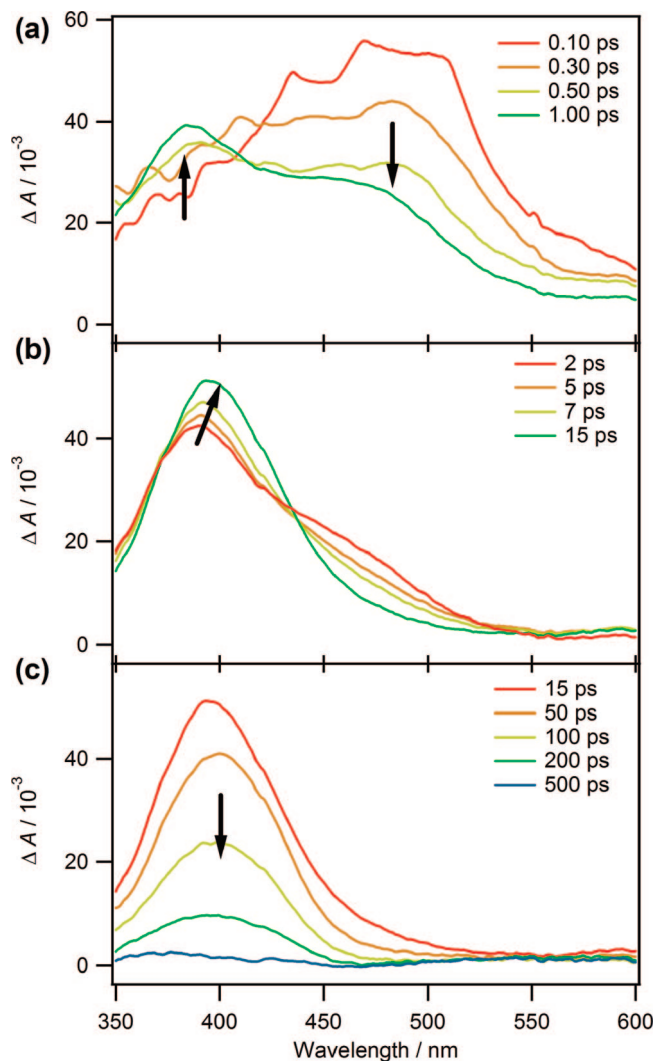


Figure 8. Transient spectra produced by ultrafast photolysis of BpCN₂COCH₃ in methanol. The spectra were generated by ultrafast LFP ($\lambda_{\text{ex}} = 308$ nm) with time windows of (a) 0.10–1.00 ps, (b) 2–15 ps, and (c) 15–500 ps.

nm (X = CH₃, $f = 0.7848$), in good agreement with the experimental results.

The experiments were repeated in diisopropyl ether which is more sterically encumbered than is THF. In this solvent, the initial absorptions of ¹BpCCO₂CH₃ and ¹BpCCOCH₃ were observed at 385 and 375 nm, respectively. Although transient absorption bands continue to grow 2–5 ps after the laser flash, unlike THF, the values of λ_{max} remain unchanged. The lifetime of ¹BpCCOCH₃ in diisopropyl ether is 310 ± 30 ps. The lifetime of ¹BpCCO₂CH₃ is too long to be resolved accurately in THF on our ultrafast spectrometer, and the best estimate of its lifetime is \sim 5 ns.

2.2.4. Halogenated Solvents. Ultrafast time-resolved studies of the two α -carbonyl diazo compounds were also performed in dichloromethane. The results in dichloromethane are similar to those obtained in acetonitrile. The data are summarized in Table 2, and the transient spectra are given in Figures S25 and S26, respectively. Both carbene spectra experience a growth at early times after the laser pulse (Figures S25a and S26a). These growths are assigned to the solvation of the carbenes following our previous studies.¹⁶ The lifetimes of the two singlet carbenes are longer in dichloromethane than in cyclohexane (Table 2).

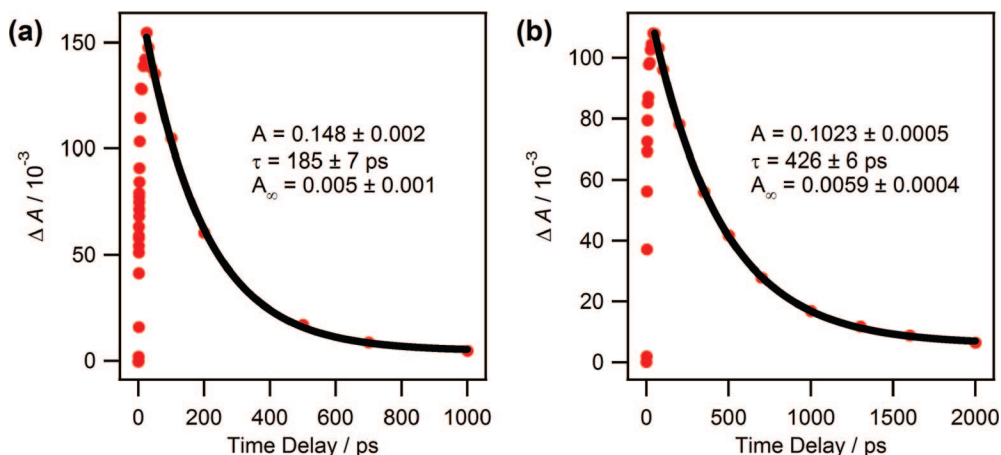


Figure 9. Kinetic traces of BpCN₂CO₂CH₃ in (a) methanol and (b) methanol-OD; excited by ultrafast LFP at 308 nm and probed at 410 nm.

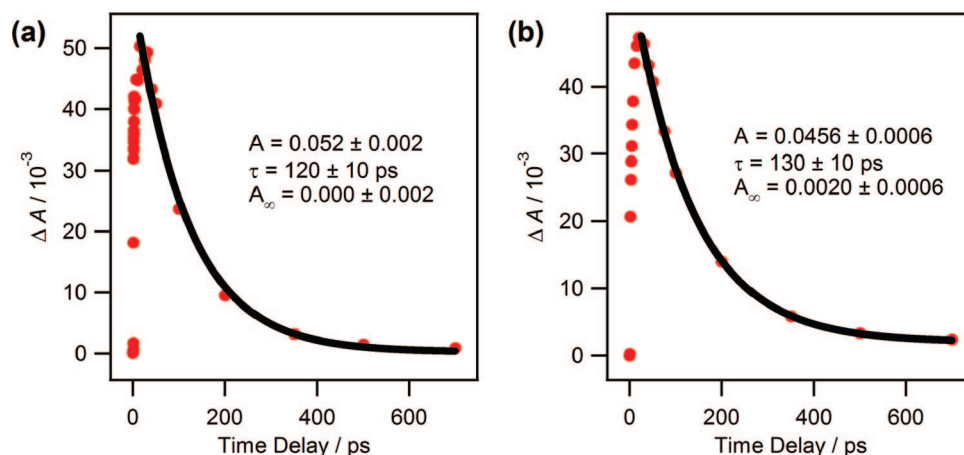


Figure 10. Kinetic traces of BpCN₂COCH₃ in (a) methanol and (b) methanol-OD; excited by ultrafast LFP at 308 nm and probed at 400 nm.

Scheme 4. Solvation Dynamics of BpCCO₂CH₃

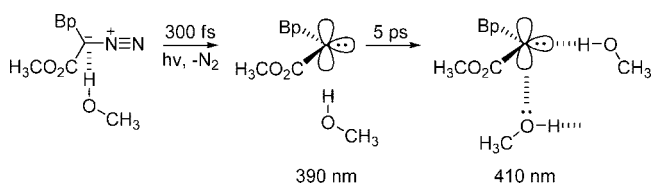


Table 3. Optical Yields of Singlet Carbenes ¹BpCCO₂CH₃ and ¹BpCCOCH₃ in Cyclohexane, Acetonitrile, and Methanol Produced by Ultrafast LFP (308 nm) of BpCN₂CO₂CH₃ and BpCN₂COCH₃^a

	¹ BpCCO ₂ CH ₃	¹ BpCCOCH ₃
cyclohexane	0.057	0.022
acetonitrile	0.065	0.030
methanol	0.077	0.040

^a Optical yields are the highest intensities of the singlet carbene bands, measured 1 ps after the laser pulse.

The lifetimes of singlet ketocarbene BpCCOCH₃ ($\lambda_{\text{max}} = 390$ nm) is 770 ± 40 ps (Figure S27) and that of the carbene ester BpCCO₂CH₃ ($\lambda_{\text{max}} = 400$ nm) are too long to measure by ultrafast spectroscopy and are in excess of several nanoseconds (Figure S26b).

With the use of ns laser flash photolysis methods, the lifetime of the carbene ester was found to be 790 ns in dichloromethane (Figure S28a) and was not affected by oxygen. As the decay of ¹BpCCO₂CH₃ proceeds, a band centered at 350 nm, which was buried under the absorption of ¹BpCCO₂CH₃, can be discerned

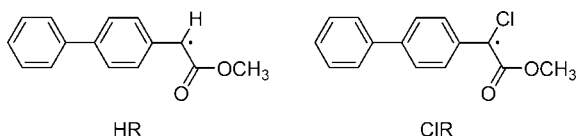
(Figure S29). The rise time of the 350 nm transient absorption cannot be determined due to its severe overlap with the spectra of ¹BpCCO₂CH₃. The decay of the 350 nm transient absorption is biexponential with two time constants of 23 and 154 μ s (Figure S30a), and the lifetimes of these species are shortened in the presence of oxygen (Figure S30b). These features suggest that the 350 nm band is a radical species. In dichloromethane-*d*₂, the lifetime of ¹BpCCO₂CH₃ is 660 ns (Figure S28b), which shows an inverse kinetic isotope effect KIE = 0.84. If a hydrogen abstraction product (HR) was formed by ¹BpCCO₂CH₃ in dichloromethane, it would have a normal KIE. The inverse KIE in dichloromethane strongly suggests the formation of radical CIR by chlorine abstraction of ¹BpCCO₂CH₃.²⁸ This is consistent with previous findings of Roth²⁹ and subsequently Jones et al.³⁰ that, in chlorinated solvents, singlet carbenes can abstract chlorine atoms and that the triplet carbene prefers to abstract hydrogen atoms. This chlorinated ester radical is also observed in CCl₄ (Figure S31). There is no evidence for radical formation in acetonitrile, where the formed transient absorbs at 340 nm (Figure S11) and its lifetime is not affected by oxygen. This transient is assigned to an ylide.

(28) Wiberg, K. B. *Physical Organic Chemistry*; Wiley: New York, 1964.

(29) Roth, H. D. *J. Am. Chem. Soc.* **1971**, *93*, 4935–4936.

(30) Jones, M. B.; Jackson, J. E.; Soundararajan, N.; Platz, M. S. *J. Am. Chem. Soc.* **1988**, *110*, 5597.

Due to the similarity of the electronic structures of HR and CIR, they are expected to have similar absorption spectra. In cyclohexane, radical HR absorbs at 335 nm (Figure S2), which as expected resembles the absorption spectra of CIR. Furthermore, TD-DFT calculations predict that CIR has an absorption at 365 nm ($f = 0.4057$, Table S9), in good agreement with the experimental data. On the basis of the inverse KIE, the absence of an oxygen-sensitive species in acetonitrile, the oxygen sensitivity of the 350 nm transient absorption, and TD-DFT calculations in the gas phase, it is safe to assign the 350 nm band to the radical CIR. We can also conclude that $^1\text{BpCCO}_2\text{CH}_3$ has a singlet ground state in dichloromethane.



3. Discussion

3.1. Wolff Rearrangements in a Diazo Excited State. Tomioka and co-workers reported product studies for the corresponding phenyl analogues of the *p*-biphenyl diazo compounds of this work.^{6,7} They found that photolysis of phenyl diazo ester $\text{PhCN}_2\text{CO}_2\text{CH}_3$ does not produce an appreciable amount of WR-derived product in alcohols.⁶ In contrast, photolysis of phenyl diazo ketone $\text{PhCN}_2\text{COCH}_3$ forms $\sim 50\%$ of WR-derived product in methanol.⁷ These results imply that the excited state of the diazo ketone undergoes WR in concert with nitrogen extrusion $\sim 50\%$ of the time, relative to other chemical processes, but that the excited state of the diazo ester does not.

Wang, Toscano, and co-workers^{5,31} studied the photochemistry of $^1\text{BpCN}_2\text{CO}_2\text{CH}_3$ using ns time-resolved infrared spectroscopy (ns-TRIR) and observed that the growth of the ketene is monoexponential in Freon-113 and proceeds with the same rate as the decay of the carbene S–T equilibrium mixture. They concluded that there is no ketene formation directly from the diazo ester singlet excited state in this solvent.

As shown in Figure S14,¹⁴ there is an instantaneous growth of the ketene band ($\tau < 0.4$ ps) upon photolysis of the *p*-biphenyl diazo ketone. The band narrows and blue-shifts over 30 ps and then grows over 700 ps, determined by ultrafast time-resolved infrared spectroscopy. In principle, the fast growth of the ketene band may be due to the formation of the ketene from “hot” $^1\text{BpCCOCH}_3$, a process which is much faster than ketene formation from thermalized $^1\text{BpCCOCH}_3$ but we expect will require ~ 10 ps. Alternatively, the ketene can be formed directly in the singlet excited state of the diazo precursor without intervention of a carbene and the 50 ps time constant is then caused by VC of the “hot” ketene. This latter mechanism is most consistent with the observation of instantaneous formation of ketenes.

A comparison of parts a and b of Figure 3 reveals that the optical yield of ketocarbene is consistently less than half of that of the carbene ester in all the solvents employed in this study (Table 3). One can simply argue that the molar absorptivity of the carbene ester is twice that of the ketocarbene. To test this possibility, TD-DFT calculations were performed on $^1\text{BpC-COCH}_3$ and $^1\text{BpCCO}_2\text{CH}_3$. These calculations predict that $^1\text{BpCCOCH}_3$ will have $\lambda_{\text{max}} = 348$ nm ($f = 0.5041$), in good

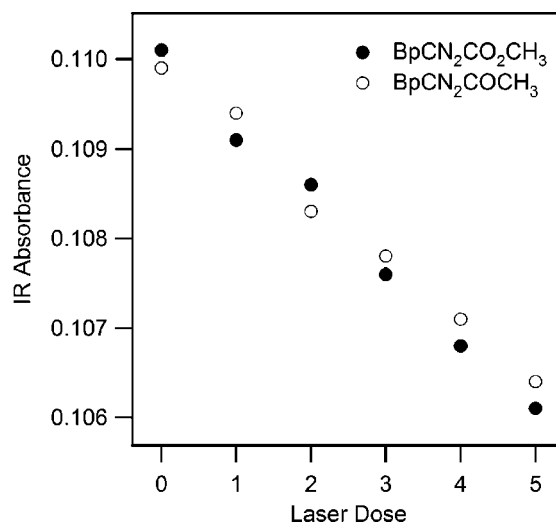


Figure 11. Decrease in diazo C=N=N IR absorbance of solutions of $\text{BpCN}_2\text{CO}_2\text{CH}_3$ and $\text{BpCN}_2\text{COCH}_3$ in acetonitrile as a function of exposure to 308 nm light from a XeCl excimer laser.

agreement with experiment. The same calculations predict that the carbene ester will have $\lambda_{\text{max}} = 368$ nm (experimental $\lambda_{\text{max}} = 375$) and $f = 0.4569$. Thus, TD-DFT calculations predict that there should not be a large difference in molar absorptivity. It is, therefore, clear that differences in molar absorptivity do not explain the optical yield data.

The data can, in principle, be explained by differences in the quantum yield of disappearance of $\text{BpCN}_2\text{COCH}_3$ and $\text{BpCN}_2\text{CO}_2\text{CH}_3$ if the former diazo compound has more efficient internal conversion than the diazo ester. To test this possibility, solutions of diazo ketone and ester in acetonitrile were prepared with identical, initial, optical densities of 1.0. Each solution was then exposed to the same number of pulses of 308 nm light from an excimer laser. As shown in Figure 11, the two diazo compounds decompose with the same quantum yield. Thus, differences in internal conversion efficiencies of the two diazo compounds do not explain the data.

To explain the data and following our previously reported studies of 1,2 hydrogen shifts in diazo excited states,¹² we posit that $^1\text{BpCN}_2\text{COCH}_3^*$ undergoes WR in competition with carbene formation to a far greater extent than the diazo ester excited state (Scheme 1). This conclusion is consistent with a large body of literature and the instantaneous ($\tau < 0.4$ ps) formation of the ketene.²

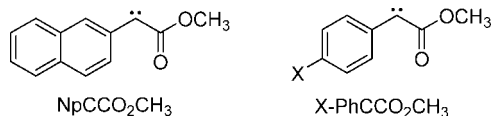
Why is there so much more WR in $^1\text{BpCN}_2\text{COCH}_3^*$ than in $^1\text{BpCN}_2\text{CO}_2\text{CH}_3^*$? One can posit, following Kaplan and Meloy,³ that the key difference resides in the syn–anti conformational equilibrium constant is more favorable to WR in the diazo ketone. Indeed inspection of Table 1 reveals that theory predicts that there is more syn diazo ketone than diazo ester at equilibrium, in the gas phase, and in the solvents of this work. The calculated differences in percent syn conformation of diazo ketone and ester at equilibrium (the conformation predicted by Kaplan and Meloy³ to be disposed to concerted WR) are significant in acetonitrile but not in cyclohexane. As the ratio of the carbene ester to keto carbene yield are the same in the two solvents the conformation of the diazo ground state cannot be the only determining factor. This is not unreasonable as nothing is currently known of the rate of syn–anti interconversion on diazo carbonyl excited-state surfaces, and it may be competitive with nitrogen extrusion (< 300 fs).

(31) Wang, Y.; Hadad, C. M.; Toscano, J. P. *J. Am. Chem. Soc.* **2002**, *124*, 1761–1767.

We speculate that a key factor is the loss of ester resonance energy that accompanies the WR of $^1\text{BpCCO}_2\text{CH}_3$. The ester resonance energy of methyl acetate is $8.5 \text{ kcal}\cdot\text{mol}^{-1}$ in the gas phase^{32,33} and is about half of that value in solution.³⁴ Thus, the WR of a diazo ester excited state will be less exothermic and slower than that of a diazo ketone excited state. The same line of reasoning predicts that the WR of a singlet ketocarbene will proceed faster than that of an analogous carbene ester (vide infra).

3.2. Carbene Intersystem Crossing and Wolff Rearrangement. Different carbene spin states have different reactivities. One must understand carbene ground-state multiplicity to fully appreciate the chemistry observed. Phenylcarbomethoxycarbene $\text{PhCCO}_2\text{CH}_3$ was first studied by Fujiwara et al.⁶ They concluded that $\text{PhCCO}_2\text{CH}_3$ has a triplet ground state in a cryogenic matrix, using electron spin resonance (ESR) spectroscopy at 77 K.⁶ The groups of Toscano and Hadad studied the S–T energy gaps of a series of para-substituted phenyl carbomethoxy carbenes $\text{PhCCO}_2\text{CH}_3$ using ns-TRIR and quantum mechanical calculations.³⁵ They discovered that an electron-donating para-substituted $\text{PhCCO}_2\text{CH}_3$ favors a singlet carbene ground state, whereas $\text{PhCCO}_2\text{CH}_3$ with an electron-withdrawing group at the para-position tends to have a triplet carbene ground state. Their experimental studies of S–T gaps as a function of solvent are consistent with their computational studies.³⁵

2-Naphthylcarbomethoxy carbene ($\text{NpCCO}_2\text{CH}_3$) has been studied extensively in cryogenic matrixes and in solution by the groups of Bally,³⁶ Toscano,⁵ Kohler,³⁷ and Platz.^{37,38} It has been reported that $\text{NpCCO}_2\text{CH}_3$ has a singlet ground state in polar solvents but a triplet ground state in nonpolar solvents.³¹



The ultrafast dynamics of $\text{NpCCO}_2\text{CH}_3$ in solution were first studied by Hess, Kohler, Likhovotvorik, Peon, and Platz (HKLPP) using femtosecond time-resolved spectroscopy.³⁷ It was reported that “all spectral evolution ceases after approximately 50 ps”, after pulsed laser photolysis, and it was concluded that 2-naphthylcarbomethoxycarbene undergoes very rapid isc (in 10 ps) in acetonitrile and in Freon-113 ($\text{CF}_2\text{ClCFCl}_2$). This is at least 1 order of magnitude faster than the isc rate found for other aryl carbenes. The authors attributed the rapid rate of isc to a coupling of the motion of ester group to the isc process.

The conclusions of HKLPP are not consistent with our observation of a rather “slow” rate of isc of $^1\text{BpCCO}_2\text{CH}_3$. We speculate that the spectrum observed by Hess et al. 50 ps after the laser pulse in acetonitrile and in Freon-113 are both purely that of the singlet carbene $^1\text{NpCCO}_2\text{CH}_3$ rather than that of the S–T carbene equilibrium mixture (Figure S32) as previously

assumed. If $^1\text{NpCCO}_2\text{CH}_3$ has an isc rate similar to that of $\text{BpCCO}_2\text{CH}_3$ ($\sim 2 \text{ ns}$), then the spectral evolution will not display significant changes on the time scale of 100–1000 ps, the longest time delay used in the study of HKLPP.³⁷

HKLPP assigned the 370 nm transient absorption band to an equilibrium mixture of singlet and triplet $\text{NpCCO}_2\text{CH}_3$ (Figure 1 of ref 37) because the ratio of the maximum absorbance of the long-wavelength band to the short-wavelength band decreases on changing the solvent from acetonitrile to Freon-113. This is the expected trend if the absorption in the long-wavelength band is primarily due to $^1\text{NpCCO}_2\text{CH}_3$ and if the equilibrium constant for S–T spin equilibration increases in the less polar solvent. For this argument to be correct, it must be based on the assumption that the ratio of the oscillator strength of the 370 and 420 nm bands of $^1\text{NpCCO}_2\text{CH}_3$ is the same in acetonitrile and in Freon-113. However, oscillator strength can vary with solvent and it is not certain that the absorbance ratio of 370 nm over 420 nm is the same for $^1\text{NpCCO}_2\text{CH}_3$ in solvents with different polarities. Given that singlet and triplet $\text{NpCCO}_2\text{CH}_3$ have similar UV spectra³⁶ (spectra b and c in Figure S33) and that $^1\text{NpCCO}_2\text{CH}_3$ is reported to be the ground state in acetonitrile,⁵ we feel it is likely that only $^1\text{NpCCO}_2\text{CH}_3$ was observed in acetonitrile instead of the S–T equilibrium mixture proposed by Hess et al.³⁷

Finally, Wang et al. deduced that the S–T gap for $\text{NpCCO}_2\text{CH}_3$ is $0.2 \pm 0.1 \text{ kcal}\cdot\text{mol}^{-1}$ in Freon-113.⁵ Ultrafast isc of $\text{NpCCO}_2\text{CH}_3$ is inconsistent with the Eisinger’s rule^{39,40} that the smaller S–T gap, the slower the rate of isc.

The S–T splitting (ΔG_{ST}) of $\text{BpCCO}_2\text{CH}_3$ was calculated as a function of solvent using DFT methods (gas phase, cyclohexane, acetonitrile, and dichloromethane). The results are given in Table 4. The S–T gaps of $\text{BpCCO}_2\text{CH}_3$ are predicted to be 2.19, 0.49, -2.72 , and $-1.94 \text{ kcal}\cdot\text{mol}^{-1}$ in the gas phase, cyclohexane, acetonitrile, and dichloromethane, respectively, where a positive sign denotes a triplet ground state and a negative sign indicates that the singlet is the ground state. On the basis of the ns LFP studies, it is clear that $\text{BpCCO}_2\text{CH}_3$ has a singlet ground state in acetonitrile and dichloromethane and a triplet ground state in cyclohexane, all of which is *qualitatively* consistent with the DFT calculations. As discussed previously, combining the ultrafast spectroscopic and ns LFP data for $\text{BpCCO}_2\text{CH}_3$ in cyclohexane, we estimate that ΔG_{ST} is within $0.4\text{--}1 \text{ kcal}\cdot\text{mol}^{-1}$ and that $^3\text{BpCCO}_2\text{CH}_3$ is the ground state in cyclohexane. The calculated S–T gap in cyclohexane is $0.49 \text{ kcal}\cdot\text{mol}^{-1}$, which is in excellent agreement with the experimental results.

The calculations consistently predict more negative S–T energy gaps for the ketocarbene relative to the carbene ester. The singlet ketocarbene is *consistently* stabilized relative to the corresponding triplet and relative to the carbene ester (Table 4). In cyclohexane, for example, the S–T splitting of the carbene ester is predicted to be $+0.49 \text{ kcal}\cdot\text{mol}^{-1}$ and that of the keto carbene is $-0.46 \text{ kcal}\cdot\text{mol}^{-1}$. Thus, if the carbene ester has a singlet ground state in a particular solvent, it seems likely that the ketocarbene will also have a singlet ground state in that solvent as well.

The lifetime of $^1\text{BpCCO}_2\text{CH}_3$ is $\sim 2 \text{ ns}$ in cyclohexane. On the basis of product studies, there is very little WR-derived

(32) Blom, C. E.; Guenthard, H. H. *Chem. Phys. Lett.* **1981**, *84*, 267–271.

(33) Wiberg, K. B.; Laidig, K. E. *J. Am. Chem. Soc.* **1987**, *109*, 5935–5943.

(34) Grindley, T. B. *Tetrahedron Lett.* **1982**, *23*, 1757–1760.

(35) Geise, C. M.; Wang, Y.; Mykhaylova, O.; Frink, B. T.; Toscano, J. P.; Hadad, C. M. *J. Org. Chem.* **2002**, *67*, 3079–3088.

(36) Zhu, Z.; Bally, T.; Stracener, L. L.; McMahon, R. J. *J. Am. Chem. Soc.* **1999**, *121*, 2863–2874.

(37) Hess, G. C.; Kohler, B.; Likhovotvorik, I.; Peon, J.; Platz, M. S. *J. Am. Chem. Soc.* **2000**, *122*, 8087–8088.

(38) Wang, J.-L.; Likhovotvorik, I.; Platz, M. S. *J. Am. Chem. Soc.* **1999**, *121*, 2883–2890.

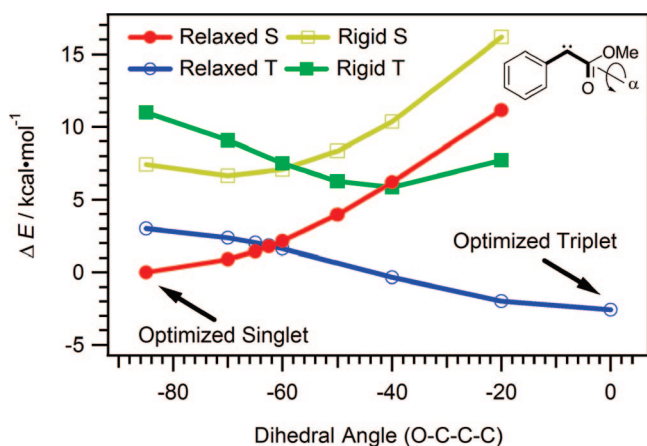
(39) Eisinger, K. B.; Turro, N. J.; Aikawa, M.; Butcher, J. A., Jr.; DuPuy, C.; Hefferon, G.; Hetherington, W.; Korenowski, G. M.; McAuliffe, M. J. *J. Am. Chem. Soc.* **1980**, *102*, 6563–6565.

(40) Sitzmann, E. V.; Langan, J.; Eisinger, K. B. *J. Am. Chem. Soc.* **1984**, *106*, 1868–1869.

Table 4. B3LYP/6-311+G(d,p)//B3LYP/6-31G(d) Calculations of Carbene Singlet–Triplet Gaps ($\text{kcal}\cdot\text{mol}^{-1}$) for $\text{BpCCO}_2\text{CH}_3$ and BpCCOCH_3 in the Gas Phase, Cyclohexane, Acetonitrile, and Dichloromethane^a

	$\text{BpCCO}_2\text{CH}_3$			BpCCOCH_3		
	$\Delta H_{\text{ST}}(\text{OK})$	$\Delta H_{\text{ST}}(298\text{K})$	$\Delta G_{\text{ST}}(298\text{K})$	$\Delta H_{\text{ST}}(\text{OK})$	$\Delta H_{\text{ST}}(298\text{K})$	$\Delta G_{\text{ST}}(298\text{K})$
gas phase ^b	1.95	2.07	2.19	−2.43	−2.75	−1.26
cyclohexane ^c	2.23	0.11	0.49	1.57	−0.70	−0.46
acetonitrile ^c	3.93	−3.05	−2.72	3.16	−4.08	−3.88
dichloromethane ^c	3.36	−2.29	−1.94	2.64	−3.28	−3.06

^a In the gas phase the energies of the fully optimized singlet and triplet carbenes are compared. The energies of the carbenes at the optimized gas-phase geometries were then recalculated in the indicated solvents. The condensed phase single-point energies of the singlet and triplet carbene are given. ^b The zero-point energy (ZPE) for the gas-phase calculations is corrected by a factor of 0.9806. The proposed energy corrections by Woodcock et al. (ref 44) were not applied on our results. ^c The solution-phase calculations used PCM models, and the geometries are from the gas-phase B3LYP/6-31(d) calculations. For the triplet carbenes, the anti conformation is more stable than the syn conformation and is used for the S–T gap calculations.

**Figure 12.** Potential energy surfaces (PES) for singlet and triplet $\text{PhCCO}_2\text{CH}_3$ in the gas phase. Relaxed $^1\text{PhCCO}_2\text{CH}_3$ PES is in red; rigid $^1\text{PhCCO}_2\text{CH}_3$ PES is in yellow; relaxed $^3\text{PhCCO}_2\text{CH}_3$ PES is in blue; rigid $^3\text{PhCCO}_2\text{CH}_3$ PES is in green. See text for more details.

product formed for photolysis of $\text{BpCN}_2\text{CO}_2\text{CH}_3$ in cyclohexane and the main product is that of solvent insertion (Scheme 3). In addition, the lifetime of $^1\text{BpCCO}_2\text{CH}_3$ is the same in cyclohexane and in cyclohexane-*d*₁₂. We conclude that the decay of $^1\text{BpCCO}_2\text{CH}_3$ in cyclohexane is mainly controlled by isc. Previous studies on diphenylcarbene,⁴¹ fluorenylidene,¹³ *p*-biphenylcarbene,¹¹ and *p*-biphenylmethylcarbene¹² show that the isc time constants in cyclohexane are no longer than 200 ps. The isc of $^1\text{BpCCO}_2\text{CH}_3$ (~2 ns) is around 1 order of magnitude slower than the previously studied carbenes.

We posit that this effect is mainly due to the significant geometry difference between singlet and triplet $\text{BpCCO}_2\text{CH}_3$. The plane of the carbonyl group of $^1\text{BpCCO}_2\text{CH}_3$ is predicted to be perpendicular to the plane of the phenyl ring. In $^3\text{BpCCO}_2\text{CH}_3$, the carbonyl group is coplanar with the phenyl ring, which imposes a dramatic structural change requirement upon the isc of $\text{BpCCO}_2\text{CH}_3$ and thus decelerates the isc rate. A potential energy surface (PES) scan was performed for $\text{PhCCO}_2\text{CH}_3$ at the B3LYP/6-311+G(d,p)//B3LYP/6-31G(d) level of theory to estimate where the singlet and triplet surfaces cross (Figure 12). A phenyl counterpart was studied instead of $\text{BpCCO}_2\text{CH}_3$ because they have similar S–T gaps in the gas phase and we assume that the substitution of biphenyl with phenyl will not alter the S–T isc barrier dramatically but will facilitate the calculations. A relaxed PES scan in the gas phase was performed for $^1\text{PhCCO}_2\text{CH}_3$ with the dihedral angle of the carbonyl group and the phenyl ring ($\alpha_{\text{O-C-C-C}}$) as the reaction

coordinate. At each relaxed geometry of $^1\text{PhCCO}_2\text{CH}_3$ along the reaction coordinate, the energies of the triplet spin isomers were calculated to search for the surface crossing between the singlet and triplet carbene PES. It was found that when $\alpha_{\text{O-C-C-C}}$ is 40° , the two PESs cross. The surface crossing point has an energy that is $6.2 \text{ kcal}\cdot\text{mol}^{-1}$ greater than that of relaxed $^1\text{PhCCO}_2\text{CH}_3$.

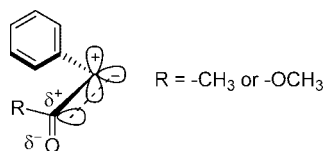
A related, relaxed PES scan was computed for $^3\text{PhCCO}_2\text{CH}_3$ with a single-point energy calculation of $^1\text{PhCCO}_2\text{CH}_3$ at each relaxed geometry of the triplet carbene. It was found that the relaxed triplet and restrained singlet PES do not cross. The smallest energy difference between these two surfaces is at $\alpha_{\text{O-C-C-C}}$ is 70° , and the restrained-to-be-planar $^1\text{PhCCO}_2\text{CH}_3$ energy is $6.7 \text{ kcal}\cdot\text{mol}^{-1}$ higher than the relaxed orthogonal $^1\text{PhCCO}_2\text{CH}_3$.

The relaxed singlet carbene PES crosses that of the relaxed triplet carbene PES at an energy that is $2 \text{ kcal}\cdot\text{mol}^{-1}$ greater than that of the relaxed $^1\text{PhCCO}_2\text{CH}_3$. We note that a barrier to isc has been reported on isc of $\text{NpCCO}_2\text{CH}_3$ in a cryogenic matrix.³⁶ Thus, based on these calculations, we conclude that if isc proceeds when the singlet and triplet carbene are isoenergetic then a barrier to isc can be estimated to vary between $\sim 2 \text{ kcal}\cdot\text{mol}^{-1}$ (if isc proceeds where the surfaces cross) to $6.7 \text{ kcal}\cdot\text{mol}^{-1}$ (if the singlet carbene must rotate to the triplet's preferred geometry to allow isc) for the isc of $^1\text{PhCCO}_2\text{CH}_3$ to its triplet. The ultimate reaction product (C–H insertion adduct, Scheme 3) must be formed from the equilibrium mixture of singlet and triplet carbene, in a process which takes longer than 2 ns.

Since Wang et al.⁵ observed ketene formation for 2- $\text{NpCCO}_2\text{CH}_3$ in acetonitrile and Freon-113, it is reasonable to assume that WR also contributes to the decay of $^1\text{BpCCO}_2\text{CH}_3$ in acetonitrile and dichloromethane where the singlet state is the ground state of the carbene. Due to other competing reactions, such as ylide formation in acetonitrile and chlorine abstraction in dichloromethane, we cannot directly deduce the WR rates in these two solvents.

DFT calculations predict that the S–T gap for BpCCOCH_3 is -1.26 , -0.46 , -3.88 , and $-3.06 \text{ kcal}\cdot\text{mol}^{-1}$ in the gas phase, cyclohexane, acetonitrile, and dichloromethane, respectively (Table 4), where the negative sign indicates a singlet ground state. The calculations predict that the S–T gap of the keto carbene is always more negative (more in favor of the singlet) than the carbene ester. The experimental evidence indicates that the carbene ester has an S–T splitting of approximately zero in cyclohexane (with a slight preference for the triplet) and a singlet ground state in acetonitrile and dichloromethane. Thus, assuming that the error in the DFT calculations are the same for $\text{BpCCO}_2\text{CH}_3$ and BpCCOCH_3 , we conclude that BpC-

(41) Peon, J.; Polshakov, D.; Kohler, B. *J. Am. Chem. Soc.* **2002**, *124*, 6428–6438.

Scheme 5. Electronic Stabilization of Carbenes by Carbonyl Groups

COCH₃ has a singlet ground state in cyclohexane, acetonitrile, and dichloromethane.

The preference of a singlet ground state for the ketocarbene as compared with the ester carbene is due to an electronic effect. The singlet carbonyl carbene geometry prefers that the carbonyl group and the plane of the phenyl ring are orthogonal (Scheme 5). A singlet carbene is much like a zwitterion. The orthogonal conformation avoids unfavorable interactions between the carbonyl group and the empty p orbital/positive charge. On the other hand, in the orthogonal conformation, the carbonyl group can stabilize the filled orbital/negative charge through conjugation. In the case of the ester carbene, stabilization of the filled orbital by the carbonyl group diminishes the resonance of the ester moiety. For the ketocarbene, the carbonyl group can better stabilize the carbene filled orbital than the carbene ester. The difference between the ketocarbene and ester carbene results in the ketocarbene always favoring a singlet carbene ground state relative to the ester carbene. The electronic effect that makes a methyl ketone more acidic than the analogous ester is the same electronic effect that favors a singlet ground state of a carbene ketone relative to a carbene ester.

Fujiwara et al.⁶ reported that triplet-sensitized photolysis of PhCN₂COCH₃ in methanol did not form appreciable yields of characteristic products of reaction of ³PhCCOCH₃, such as double hydrogen abstraction product. This observation is consistent with a singlet ground state for PhCCOCH₃ in this solvent. Nanosecond laser flash photolysis of BpCN₂COCH₃ also did not provide evidence for the formation of the triplet carbene (Figure S9). On the basis of the ultrafast results, the decay of ¹BpCCOCH₃ is a unimolecular process, either WR or isc, or both. Since DFT calculations predict singlet ground states for BpCCOCH₃, the rate of an uphill isc process will be slow. Thus, we conclude that ¹BpCCOCH₃ mainly decays by WR in cyclohexane, acetonitrile, and dichloromethane. WR must proceed faster in a nonpolar solvent cyclohexane ($\tau = 180$ ps) than in a polar solvent acetonitrile ($\tau = 700$ ps). This may be due to the fact that the singlet carbene is more polar than the transition state of WR. Assuming an Arrhenius pre-exponential factor of WR is 10¹³, one can deduce the activation barrier of WR for ¹BpCCOCH₃ is 4.4 and 5.2 kcal·mol⁻¹ in cyclohexane and acetonitrile, respectively. The group of Radom⁴ calculated the WR barriers for parent formyl carbene to be 2.4–7.2 kcal·mol⁻¹ in the gas phase. We performed B3LYP/6-31(d) calculations and obtained WR barriers of 4.4 and 8.9 kcal·mol⁻¹ for the *p*-biphenyl keto carbene and *p*-biphenyl carbene ester, respectively, in the gas phase (Table 5). Our calculations reveal that the barriers to WR of the arylketone are similar to that calculated for formylcarbene and are in excellent agreement with our experimental values for the barrier to WR of ¹BpCCOCH₃. The greater calculated barrier to WR of the carbene ester is attributed to the loss of ester resonance energy in the WR of ¹BpCCO₂CH₃. Our calculations also explain why the lifetime of the keto carbene is shorter than that of the analogous carbene ester in acetonitrile, THF, and dichloromethane.

However, in the halogenated solvent dichloromethane, the WR rate of the ketocarbene is comparable to that of the same carbene in acetonitrile. On the basis of the $E_T(30)$ values, dichloromethane is more polar than cyclohexane but less polar than acetonitrile. The comparable WR rate in acetonitrile and dichloromethane suggests that the rate of WR in solution is not simply controlled by solvent polarity. We have reported a halogenated solvent effect on the isc rates of certain carbenes with triplet ground states.¹⁷ This was attributed to coordination of the carbene with the halogenated solvent. We propose that the same type of coordination of ¹BpCCOCH₃ with acetonitrile and dichloromethane (solvent nonbonding electron pairs with the empty p orbital of the singlet carbene) stabilizes the ketocarbene and depresses the rate of WR in these solvents relative to cyclohexane.

4. Experimental Section

4.1. Calculations. DFT and TD-DFT calculations were performed using the Gaussian 03 suite of programs at The Ohio Supercomputer Center.⁴² For the gas-phase calculations, geometries were optimized at the B3LYP/6-31G(d) level of theory with single-point energies obtained at the B3LYP/6-311+G(d,p)//B3LYP/6-31G(d) level of theory. Vibrational frequency analyses at the B3LYP/6-31G(d) level were utilized to verify that stationary points obtained corresponded to energy minima. All the transition states have one and only one imaginary frequency. The zero-point energy (ZPE) was corrected with a factor of 0.9806. The solution-phase calculations used PCM models and were performed at B3LYP/6-311+G(d,p)(PCM)//B3LYP/6-31G(d)(gas phase) level of theory (refer to the footnotes of tables). The electronic spectra were computed using time-dependent density functional theory with Gaussian 03 at the B3LYP/6-311+G(d,p) level and using the B3LYP/6-31G(d) geometry; for these calculations, 20 allowed electronic transitions were calculated. Carbonyl carbenes and their derivatives have *s*-Z and *s*-E conformations. Both conformers were calculated for each species, and the most stable conformers were shown and used to calculate the electronic spectra.

4.2. Ultrafast Spectroscopy. Ultrafast UV–vis broad-band absorption measurements were performed using the home-built spectrometer described previously.²³ Samples were prepared in 50 mL of solvent with absorption 1.0 at the excitation wavelength with 1.0 mm optical length. For the bleaching control experiments (cf., section 4.3), the bleached solutions for BpCN₂CO₂CH₃ and BpCN₂COCH₃ in acetonitrile were prepared with the same concentration as in their corresponding ultrafast experiments, bleached using a 308 nm excimer laser for 10 min, and ultrafast spectroscopic experiments were then performed immediately to avoid decomposition of unstable photoproducts.

The ultrafast infrared laser system (see Scheme S1 of the Supporting Information) consists of a short-pulse titanium–sapphire oscillator (Coherent, Mira) followed by a high-energy titanium–sapphire regenerative amplifier (Coherent, Positive Light, Legend HE USP). The beam is split into two beams to pump two OPAs (OPeA Coherent). The OPA with an SFG module generates a UV pump pulse (tunable from 240 to 310 nm), while the second OPA has a DFG module producing IR pulses (tunable from 2 to 10 μ m). A Ge beamsplitter splits the IR beam into reference and probe beams, and both are focused into the sample cell (Harrick Scientific), but only the probe beam overlaps with the pump beam in the sample. After passing through the sample the probe and reference beams were spectrally dispersed in a grating spectrometer (Triax 320) and independently imaged on a liquid nitrogen cooled HgCdTe detector (2 × 32 elements) with 17 nm resolution. Every second UV pump pulse is blocked by a synchronized chopper to eliminate long-term

(42) Frisch, M. J.; et al. *Gaussian 03*, revision C.02; Gaussian, Inc.: Wallingford, CT, 2004.

Table 5. B3LYP/6-31G(d) Calculations of Relative Energies of the Transition State and the Product of Wolff Rearrangement ($\text{kcal}\cdot\text{mol}^{-1}$) for $^1\text{BpCCO}_2\text{CH}_3$ and $^1\text{BpCCOCH}_3$ in the Gas Phase^a

	$\text{BpCCO}_2\text{CH}_3$			BpCCOCH_3		
	$\Delta H_{\text{ST(OK)}}$	$\Delta H_{\text{ST(298K)}}$	$\Delta G_{\text{ST(298K)}}$	$\Delta H_{\text{ST(OK)}}$	$\Delta H_{\text{ST(298K)}}$	$\Delta G_{\text{ST(298K)}}$
WR T.S.	8.92	8.79	8.88	3.67	3.27	4.40
ketene	−29.08	−29.14	−28.74	−51.22	−51.54	−50.51

^a The zero-point energy (ZPE) for the gas-phase calculations is corrected by a factor of 0.9806. The energies are relative to its corresponding carbene singlet state.

drift effects. Solution concentrations were adjusted to an absorption of 0.7 in a 1 mm cell at the excitation wavelength. The pump pulse energy was about 4 μJ at the sample position. The entire set of pump–probe delay positions (cycle) is repeated at least three times, to observe data reproducibility from cycle to cycle. To avoid rotational diffusion effects, the angle between polarizations of the pump beam and the probe beam was set to the magic angle (54.7°). Kinetic traces are analyzed by fitting to a sum of exponential terms. Convolution with a Gaussian response function is included in the global fitting procedure. The instrument response was approximately 300 fs (fwhm). All the experiments were performed at room temperature.

4.3. Re-excitation of Persistent Photoproducts. An enigmatic band is observed at 480 nm in the study $\text{BpCN}_2\text{CO}_2\text{CH}_3$ in acetonitrile. The lifetime of this transient absorption is hundreds or thousands of picoseconds. A sample of the diazo compound in acetonitrile was bleached with pulses of 308 nm excimer laser light, and then the bleached solution was immediately studied by ultrafast spectroscopic techniques. Pulsed laser photolysis of the bleached solution does produce the 480 nm transient (Figure S34); thus, the carrier of this species does not originate from the primary photochemistry of the diazo compound. The bleached solution does not produce a transient absorption at 400 nm, indicating that the 400 nm transient absorption, which is assigned to the carbene, is not due to re-excitation of reaction products.

Similarly, re-excitation was also performed in the case of $\text{BpCN}_2\text{COCH}_3$. In acetonitrile, there was a shoulder observed at 440 nm upon photolysis of bleached solution. In cyclohexane, a transient absorption centered at 500 nm was visible. Ultrafast spectroscopic studies of bleached $\text{BpCN}_2\text{COCH}_3$ in acetonitrile produces two transients, centered at 440 and 500 nm (Figure S35), suggesting the 440 and 500 nm transient absorptions are due to re-excitation. This photolysis of the bleached solution does not produce a transient absorbing at 370 nm, assuring the transient observed at 370 nm is due to the primary photochemistry of the diazo compound.

4.4. Synthesis and Product Studies. All materials and solvents were purchased from Aldrich. The solvents for ultrafast studies were spectrophotometric grade from Aldrich and used as received.

4.5. Methyl *p*-Biphenylacetate. A 200 mL flask is charged with 2.12 g of biphenylacetic acid (10.0 mmol) and 0.95 mL of dimethyl sulfate (10.0 mmol). The flask is cooled in an ice bath, and 1.8 mL of DBU (12.0 mmol) is added dropwise. The solution is stirred for 4 h, and TLC is used to monitor the completion of the reaction. Methanol is removed under vacuum. The crude material is run through a short column using dichloromethane as eluent. The solvent is removed under vacuum, and a white, solid product is afforded (2.26 g, yield 100%). ^1H NMR (500 MHz, CDCl_3): δ 7.55–7.59 (m, 4 H), 7.42–7.45 (m, 2H), 7.32–7.37 (m, 3H), 3.72 (s, 3H), 3.68 (s, 2H).

4.6. Methyl 2-(biphenyl-4-yl)-2-diazoacetate ($\text{BpCN}_2\text{CO}_2\text{CH}_3$). Methyl biphenylacetate (0.226 g, 1.0 mmol) and tosyl azide (0.197 g, 1.0 mmol) are dissolved in 10 mL of dichloromethane. DBU (0.3 mL, 2.0 mmol) is added to the solution dropwise at 0°C , and the mixture is stirred overnight. The reaction is quenched by saturated ammonium chloride solution, washed by brine, and dried by sodium sulfate. The solvent is removed under vacuum. The crude material is purified by column chromatography with a mixture of pentane and dichloromethane (1:1). An orange crystal

is formed (0.15 g, yield 60%). ^1H NMR (500 MHz, CDCl_3): δ 7.62–7.64 (m, 2H), 7.59–7.61 (m, 2H), 7.55–7.56 (m, 2H), 7.43–7.46 (m, 2H), 7.33–7.36 (m, 1H), 3.89 (s, 3H). ^{13}C NMR (125 MHz, CDCl_3): δ 165.6, 140.3, 138.7, 128.8, 127.6, 127.4, 127.1, 126.9, 124.3, 124.3, 52.1.

4.7. *p*-Biphenylacetone. A 50 mL flask is charged with 2.12 g of biphenylacetic acid (10.0 mmol), 3.6 mL of thionyl chloride (50 mmol), and 20 mL of dichloromethane. The solution is refluxed overnight, and the solvent and excess thionyl chloride are removed under vacuum to afford biphenylacetic chloride. Biphenylacetic chloride is dissolved in 20 mL of dichloromethane and 1.07 g of *N,O*-dimethylhydroxylamine hydrochloride (11.0 mmol). The solution is cooled in an ice bath, and 4.5 mL of DBU is added dropwise. The reaction is monitored by GC–MS. The reaction mixture is washed by saturated ammonium chloride (10 mL \times 2), then water (10 mL), and dried with sodium sulfate. The solvent is removed under vacuum to afford $\text{BpCH}_2\text{CON}(\text{OCH}_3)\text{CH}_3$, where Bp = biphenyl. $\text{BpCH}_2\text{CON}(\text{OCH}_3)\text{CH}_3$ is dissolved in 30 mL of anhydrous THF, and 5 mL of 3 M CH_3MgCl solution is added dropwise at 0°C over 1 h. The reaction mixture is stirred for 4 h and monitored by GC–MS. Upon completion of the reaction, it is quenched by saturated ammonium chloride solution and washed by brine. The solvent is removed under vacuum. The crude material is purified by column chromatography with a mixture of pentane and ether (10:1). White solid is afforded (1.26 g, yield 60%). ^1H NMR (500 MHz, CDCl_3): δ 7.56–7.59 (m, 4H), 7.42–7.45 (m, 2H), 7.33–7.36 (m, 1H), 7.27–7.29 (m, 2H), 3.74 (s, 2H), 2.20 (s, 3H).

4.8. 1-(Biphenyl-4-yl)-1-diazopropan-2-one ($\text{BpCN}_2\text{COCH}_3$). *p*-Biphenylacetone (0.210 g, 1.0 mmol) and tosyl azide (0.197 g, 1.0 mmol) are dissolved in 10 mL of dichloromethane. DBU (0.3 mL, 2.0 mmol) is added to the solution dropwise at 0°C , and the mixture is stirred overnight. The reaction is quenched by saturated ammonium chloride solution, washed by brine, and dried by sodium sulfate. The solvent is removed under vacuum. The crude material is purified by column chromatography with a mixture of pentane and dichloromethane (1:1). Orange crystal is afforded (0.14 g, yield 60%). ^1H NMR (500 MHz, CDCl_3): δ 7.64–7.66 (m, 2H), 7.57–7.61 (m, 4H), 7.43–7.47 (m, 2H), 7.34–7.38 (m, 1H), 2.41 (s, 3H). ^{13}C NMR (125 MHz, CDCl_3): δ 140.2, 139.8, 128.9, 127.7, 127.5, 126.9, 124.3, 27.0.

4.9. ^1H NMR and GC–MS Analysis of Photolysis Mixtures for $\text{BpCN}_2\text{CO}_2\text{CH}_3$ (Scheme 3). Photolysis of $\text{BpCN}_2\text{CO}_2\text{CH}_3$ was performed in cyclohexane using a 10 Hz excimer laser (XeCl, 308 nm, 17 ns, ~ 0.5 J/pulse) source for 5 min. In a quartz cuvette, 3.1 mg of $\text{BpCN}_2\text{CO}_2\text{CH}_3$ was dissolved in 2.48 g of cyclohexane (~ 3.9 mM). The sample solution was purged with argon for 5 min before photolysis. During photolysis, the sample solution was shaken and argon was bubbled through the solution. The completion of the photolysis was monitored by UV–vis spectroscopy. After photolysis, 0.5 mL of ethanol was added immediately to quench formation of any ketene. The solvent was removed under vacuum, and the product mixture was dissolved in CD_2Cl_2 and analyzed by ^1H NMR (400 MHz). Note that CD_2Cl_2 was used instead of CDCl_3 because CHCl_3 impurity has a signal at 7.26 ppm, which may overlap with the signals of the biphenyl moiety and complicate the integration. We assumed that the products derived from $\text{BpCN}_2\text{CO}_2\text{CH}_3$ will have an intact biphenyl ring system. The

aromatic hydrogens (δ 7.2 to \sim 8.0) were integrated and defined as the total yield (100%). The NMR peaks in the mixture were identified either by comparison with authentic samples or the literature NMR data of the same compound or their monophenyl counterparts in the literature. Generally speaking, changing from phenyl to biphenyl should only change the chemical shifts of their nonconjugated substituents downfield by less than 0.1 ppm, such as toluene (CH_3 , δ 2.34) and *p*-phenyltoluene (CH_3 , δ 2.39), acetophenone (CH_3 , δ 2.59), and *p*-phenylacetophenone (CH_3 , δ 2.61). On the basis of this rule and the NMR literature data of the phenyl counterparts, the chemical shifts of the biphenyl photoproducts can be reasonably estimated.

The photolysis mixture was also analyzed by GC–MS. The WR product was not observed either by NMR or by GC–MS analysis. Two major peaks were observed by GC–MS, with retention times (RT) of 8.45 and 12.25 min. The mass spectrum of the component with RT of 8.45 min has a molecular ion peak at m/z 226. This is assigned to methyl *p*-biphenylacetate, which is formed by double hydrogen abstraction of $^3\text{BpCCO}_2\text{CH}_3$ from cyclohexane. This assignment is also confirmed by comparing the MS fragmentation pattern of its phenyl counterpart in the literature.⁴³ The MS of the component with RT of 12.25 min has a base peak at m/z 226, which is also the peak with the highest mass observed. The fragmentation pattern of this component is different from that of the RT 8.45 min component. The component with RT of 12.25 min is assigned to the carbene–cyclohexane adduct. The m/z 226 peak in MS is formed by a McLafferty rearrangement.

Some minor components were observed by GC–MS. The component with a RT of 5.30 min ($m/z_{\text{M}^+} = 166$) is assigned to bicyclohexyl, and the MS spectrum is consistent with that reported in the literature.⁴³

The analogous photolysis was performed for $\text{BpCN}_2\text{CO}_2\text{CH}_3$ in a 1:1 mixture of cyclohexane–cyclohexane- d_{12} , and the reaction mixture was analyzed by GC–MS. There are three major components observed with RTs of 8.45, 12.15, and 12.23 min. The component with RT of 8.45 min is assigned to methyl *p*-biphenylacetate based on our previous analysis. The components with RTs of 12.15 and 12.23 min were assigned to the adducts of $\text{BpCCO}_2\text{CH}_3$ –cyclohexane- d_{12} (base peak $m/z = 228$) and $\text{BpCCO}_2\text{CH}_3$ –cyclohexane (base peak $m/z = 226$), respectively. The area ratio between the peaks for $\text{BpCCO}_2\text{CH}_3$ –cyclohexane and $\text{BpCCO}_2\text{CH}_3$ –cyclohexane- d_{12} is 2.5.

5. Conclusions

Photolysis of $\text{BpCN}_2\text{CO}_2\text{CH}_3$ produces the excited state of this compound ($\lambda_{\text{max}} = 480$ nm) within the instrument response. The excited state decomposes to form singlet *p*-biphenyl carbomethoxy carbene ($\text{BpCCO}_2\text{CH}_3$). This carbene has a singlet ground state at ambient temperature in acetonitrile and in dichloromethane as their lifetimes are hundreds of nanoseconds

in these solvents and have no sensitivity to the presence of oxygen. In acetonitrile, the singlet ester carbene lifetime is mainly controlled by $\text{ACN}-\text{Y}$ ylide formation. In dichloromethane, $^1\text{BpCCO}_2\text{CH}_3$ abstracts a chlorine atom to form a radical pair. In cyclohexane, $^3\text{BpCCO}_2\text{CH}_3$ is the ground state and the lifetime of $^1\text{BpCCO}_2\text{CH}_3$ is controlled by isc ($\tau \sim 2$ ns) based on the spectroscopic data and product studies. The slow isc rate is due to the need for the singlet carbene to rotate to a high-energy conformation to allow relaxation. In methanol, TFE, and THF, reactions with solvent control the fate of $^1\text{BpCCO}_2\text{CH}_3$ and form O–H insertion product, cation $\text{BpCHCO}_2\text{CH}_3^+$ and THF–Y ylide, respectively.

The optical yields of the ketocarbene $^1\text{BpCCOCH}_3$ are much lower than that of the carbene ester $^1\text{BpCCO}_2\text{CH}_3$, from which we conclude that Wolff rearrangement in the excited state of the diazoketone is a more significant process than the analogous process in the excited state of the diazo ester. This is attributed to the loss of ester resonance in the Wolff rearrangement of the excited diazo ester which makes it a less exothermic and slower process.

On the basis of DFT calculations and experimental results, we conclude that $^1\text{BpCCOCH}_3$ has a singlet ground state in cyclohexane, acetonitrile, and dichloromethane. The lifetime of $^1\text{BpCCOCH}_3$ is shorter than that of $^1\text{BpCCO}_2\text{CH}_3$ in all the solvents employed in this study except TFE. The lifetime of $^1\text{BpCCOCH}_3$ is controlled by Wolff rearrangement in cyclohexane, acetonitrile, and dichloromethane. The rate of Wolff rearrangement of the ketocarbene is faster in cyclohexane than in acetonitrile and dichloromethane. Solvent coordination stabilizes the carbene and depresses the rate of Wolff rearrangement. The lifetime of $^1\text{BpCCOCH}_3$ is the same in methanol and in methanol–OD, indicating the deactivation of this singlet carbene is mainly controlled by the formation of $\text{MeOH}-\text{Y}$ ylide, which is followed by an ultrafast proton shuttle to form an ether. In THF, the THF–Y ylide formation is also observed for $^1\text{BpCCOCH}_3$.

Acknowledgment. Support of the CCBd and of this project by the National Science Foundation is gratefully acknowledged along with the support of the Ohio Supercomputer Center. J.W. gratefully acknowledges an Ohio State University Presidential Fellowship. G.B. thanks Foundation for Polish Science and MF EOG for a “Homing” Grant in the year 2008. The authors thank Professor C. M. Hadad with guidance on the calculations performed.

Supporting Information Available: Spectra and kinetics of ultrafast studies and TD-DFT calculations. Complete ref 42. This material is available free of charge via the Internet at <http://pubs.acs.org>.

JA803096P

(43) National Institute of Advanced Industrial Science and Technology. SDBS Web: <http://riodb01.ibase.aist.go.jp/sdbs/>.

(44) Woodcock, H. L.; Moran, D.; Brooks, B. R.; Schleyer, P. v. R.; Schaefer, H. F. J. *Am. Chem. Soc.* **2007**, *129*, 3763–3770.